CHAPTER FIVE

Time-Domain Analysis

The previous chapter dealt with the solution of the MTL equations for the case of *sinusoidal steady-state* excitation of the line; that is, the sources are sinusoids at a single frequency and are assumed to have been applied for a sufficiently long time such that all transients have decayed to zero leaving only the steady-state solution. In this chapter we will examine the *total* solution of the MTL equations for *general time variation of the sources.* This solution will include both the transient and the steady-state components of the solution and will apply for arbitrary, time-domain excitation signals.

It is important to understand the relative solution difficulty for the various classes of *uniform lines* at the outset. In the case of the frequency-domain solution, we have seen in the previous chapter that the solution of the MTL equations is a straightforward process whether the line is lossless *or* lossy! We will see in this chapter that the time-domain solution of the MTL equations for a *lossless line* is also a straightforward computational process! Conductors exhibit a frequency-dependent resistance and internal inductance due to the skin effect. This dependence on frequency is $\sqrt{f}$ which is difficult to characterize in the time domain. Incorporation of these losses into the frequency-domain solution is trivial; compute the resistance and internal inductance at the frequency of interest, include them as constants in the MTL equations and solve them. For the next frequency of interest, recompute the resistance and internal inductance for this frequency and repeat the solution. Typically the loss introduced by a nonzero conductivity of the surrounding media is not as significant as the loss introduced by imperfect conductors although it can be easily incorporated into the frequency-domain solution. Although the inclusion of these skin-effect losses does not significantly complicate the frequency-domain solution, it adds considerable complications to the general, time-domain solution of the MTL equations.

The additional complication in the time-domain solution over the frequency-domain solution for *lossy lines* is the *decoupling* of the MTL equations. In the frequency-domain solution, we determine an $n \times n$ transformation matrix,

$\hat{\mathbf{T}}$, that simultaneously diagonalizes *two* complex-valued matrices, $\hat{\mathbf{Z}}(\omega) = \mathbf{R}(\omega) + j\omega\mathbf{L}$, and $\hat{\mathbf{Y}}(\omega) = \mathbf{G}(\omega) + j\omega\mathbf{C}$ although we can frequently ignore the losses in the medium contained in **G**. In the case of the time-domain solution for *lossless lines*, in order to decouple the MTL equations we must determine an $n \times n$ transformation matrix, **T**, that simultaneously diagonalizes only *two* matrices, **L** and **C**. Because **L** and **C** are real, symmetric, and positive definite, this is always possible as we showed in the previous chapter. In the case of the time-domain solution for *lossy lines*, in order to decouple the MTL equaations we must determine an $n \times n$ transformation matrix, **T**, that simultaneously diagonalizes *three* matrices, **R**, **L**, and **C**. In general, this is not possible! So the decoupling of the MTL equations for the time-domain analysis of *lossy lines* is not a viable technique.

We begin the discussion with a review of the solution for two-conductor, lossless lines. This serves to introduce the notion of traveling waves on the line and also introduces an important solution technique for numerical computation: the method of characteristics or Branin's method. Next we discuss the solution of the MTL equations for lossless lines. And finally, we tackle the difficult problem of the time-domain solution of the MTL equations for lossy lines.

5.1 TWO-CONDUCTOR LOSSLESS LINES

The scalar transmission-line equations for two-conductor lossless lines are

$$\frac{\partial V(z, t)}{\partial z} = -l\frac{\partial I(z, t)}{\partial t} \tag{5.1a}$$

$$\frac{\partial I(z, t)}{\partial z} = -c\frac{\partial V(z, t)}{\partial t} \tag{5.1b}$$

Differentiating one equation with respect to z and the other with respect to t and substituting yields the uncoupled, second-order differential equations

$$\frac{\partial^2 V(z, t)}{\partial z^2} = lc\frac{\partial^2 V(z, t)}{\partial t^2} \tag{5.2a}$$

$$\frac{\partial^2 I(z, t)}{\partial z^2} = cl\frac{\partial^2 I(z, t)}{\partial t^2} \tag{5.2b}$$

The solutions to these equations are [A.1]

$$V(z, t) = V^+\left(t - \frac{z}{v}\right) + V^-\left(t + \frac{z}{v}\right) \tag{5.3a}$$

$$I(z, t) = I^+\left(t - \frac{z}{v}\right) + I^-\left(t + \frac{z}{v}\right) \tag{5.3b}$$
$$= \frac{1}{Z_C} V^+\left(t - \frac{z}{v}\right) - \frac{1}{Z_C} V^-\left(t + \frac{z}{v}\right)$$

where the *characteristic impedance* is

$$Z_C = \sqrt{\frac{l}{c}} \tag{5.4}$$
$$= vl$$
$$= \frac{1}{vc}$$

and the *velocity of propagation* of the forward-traveling waves, V^+, and backward-traveling waves, V^-, is

$$v = \frac{1}{\sqrt{lc}} \tag{5.5}$$

The functions of t and z, $V^+(t, z)$ and $V^-(t, z)$, are as yet unknown but have time and position related *only as* $t \pm z/v$.

As an alternative method of obtaining this general solution that will prove useful in our later results, let us obtain the *Laplace transform* of the transmission-line equations [A.2]. Denoting the Laplace transform of the voltage and current with respect to the time variable as $V(z, s)$ and $I(z, s)$ where s is the Laplace transform variable, the transmission-line equations in (5.1) become

$$\frac{d}{dz} V(z, s) = -slI(z, s) \tag{5.6a}$$

$$\frac{d}{dz} I(z, s) = -scV(z, s) \tag{5.6b}$$

The uncoupled second-order equations in (5.2) become

$$\frac{d^2}{dz^2} V(z, s) = s^2 lcV(z, s) \tag{5.7a}$$

$$\frac{d^2}{dz^2} I(z, s) = s^2 clI(z, s) \tag{5.7b}$$

The general solutions to these equations are

$$V(z, s) = V^+(s)e^{-sz/v} + V^-(s)e^{sz/v} \tag{5.8a}$$

$$I(z, s) = I^+(s)e^{-sz/v} + I^-(s)e^{sz/v} \tag{5.8b}$$

$$= \frac{1}{Z_C} V^+(s)e^{-sz/v} - \frac{1}{Z_C} V^-(s)e^{sz/v}$$

This is equivalent to the spectral-domain method of solving Laplace's equation discussed in Chapter 3 wherein the transform with respect to one of the independent variables converts the partial differential equations into ordinary differential equations. The inverse Laplace transform of these results can be easily obtained by recognizing the fundamental time-delay result [A.2]:

$$F(s)e^{\pm as} \Leftrightarrow f(t \pm a) \tag{5.9}$$

Applying this to (5.8) with a corresponding to z/v again gives the general form of the solution in (5.3).

The Laplace-transformed chain parameter matrix obtained in the previous chapter can be obtained from the frequency-domain result derived there and given, for a lossless line, by (4.23) with $\gamma = j\beta$:

$$\hat{V}(\mathscr{L}) = \cos(\beta\mathscr{L})\hat{V}(0) - jZ_C \sin(\beta\mathscr{L})\hat{I}(0) \tag{5.10a}$$

$$\hat{I}(\mathscr{L}) = -j\frac{1}{Z_C}\sin(\beta\mathscr{L})\hat{V}(0) + \cos(\beta\mathscr{L})\hat{I}(0) \tag{5.10b}$$

where $\beta = \omega/v$. The chain parameters relate the *phasor* voltages and currents at the two ends of the line. The Laplace-transformed result can be obtained by simply replacing $j\omega$ with s and assuming the line is *initially relaxed* so that $V(z, t) = I(z, t) = 0$ for all $0 \le z \le \mathscr{L}$ and $t \le 0$. Recalling the definitions of cosine and sine and replacing $j\omega$ with s in those relations:

$$\cos(\beta\mathscr{L}) = \frac{e^{j\omega\mathscr{L}/v} + e^{-j\omega\mathscr{L}/v}}{2} \Leftrightarrow \frac{e^{sT} + e^{-sT}}{2} \tag{5.11a}$$

$$j\sin(\beta\mathscr{L}) = \frac{e^{j\omega\mathscr{L}/v} - e^{-j\omega\mathscr{L}/v}}{2} \Leftrightarrow \frac{e^{sT} - e^{-sT}}{2} \tag{5.11b}$$

gives

$$V(\mathscr{L}, s) = \left(\frac{e^{sT} + e^{-sT}}{2}\right)V(0, s) - Z_C\left(\frac{e^{sT} - e^{-sT}}{2}\right)I(0, s) \tag{5.12a}$$

$$I(\mathscr{L}, s) = -\frac{1}{Z_C}\left(\frac{e^{sT} - e^{-sT}}{2}\right)V(0, s) + \left(\frac{e^{sT} + e^{-sT}}{2}\right)I(0, s) \tag{5.12b}$$

where we have defined the *one-way delay* of the line as

$$T = \frac{\mathscr{L}}{v} \tag{5.13}$$

The time-domain result can be obtained by applying the basic time-delay Laplace transform pair given in (5.9) to (5.12) to give

$$\begin{aligned} V(\mathscr{L}, t) &= \tfrac{1}{2}V(0, t+T) + \tfrac{1}{2}V(0, t-T) - \tfrac{1}{2}Z_C I(0, t+T) + \tfrac{1}{2}Z_C I(0, t-T) \qquad (5.14a) \\ &= \tfrac{1}{2}[V(0, t+T) - Z_C I(0, t+T)] + \tfrac{1}{2}[V(0, t-T) + Z_C I(0, t-T)] \end{aligned}$$

$$\begin{aligned} I(\mathscr{L}, t) &= -\frac{1}{2}\frac{1}{Z_C}V(0, t+T) + \frac{1}{2}\frac{1}{Z_C}V(0, t-T) + \tfrac{1}{2}I(0, t+T) \qquad (5.14b) \\ &\quad + \tfrac{1}{2}I(0, t-T) \\ &= \frac{1}{2}\left[-\frac{1}{Z_C}V(0, t+T) + I(0, t+T)\right] + \frac{1}{2}\left[\frac{1}{Z_C}V(0, t-T) + I(0, t-T)\right] \end{aligned}$$

This latter result will prove useful in subsequent work. It relates the voltage and current at $z = \mathscr{L}$, $V(\mathscr{L}, t)$, and $I(\mathscr{L}, t)$, to those values at $z = 0$, $V(0, t)$, and $I(0, t)$, that are either *delayed in time by one time delay*, $V(0, t - T)$ and $I(0, t - T)$, or are *advanced in time by one time delay*, $V(0, t + T)$ and $I(0, t + T)$. These can be placed in another form by multiplying (5.14b) by Z_C and adding and subtracting (5.14a) and (5.14b) to give

$$V(\mathscr{L}, t) + Z_C I(\mathscr{L}, t) = V(0, t - T) + Z_C I(0, t - T) \tag{5.15a}$$

$$V(\mathscr{L}, t) - Z_C I(\mathscr{L}, t) = V(0, t + T) - Z_C I(0, t + T) \tag{5.15b}$$

These can also be time shifted to yield

$$V(\mathscr{L}, t) + Z_C I(\mathscr{L}, t) = V(0, t - T) + Z_C I(0, t - T) \tag{5.16a}$$

$$V(\mathscr{L}, t - T) - Z_C I(\mathscr{L}, t - T) = V(0, t) - Z_C I(0, t) \tag{5.16b}$$

Equations (5.16) will form the basis of a very effective method of solution of the MTL equations for *lossless lines* that is referred to as the *method of characteristics* or *Branin's method.* It is important to point out that all of the above transform solution methods and results can be directly translated to the solution of the MTL equations for a uniform, multiconductor, *lossless* transmission consisting of any number of conductors. So we see why the analysis of *lossless* MTL's will be a straightforward task.

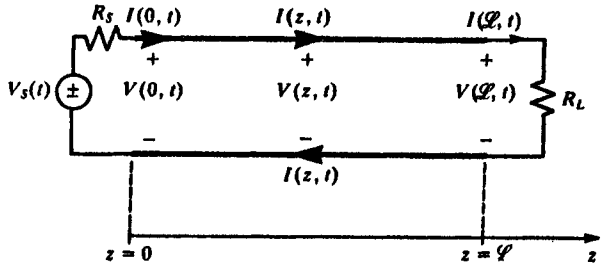

FIGURE 5.1 A two-conductor line in the time domain.

5.1.1 Graphical Solutions

We will again consider lines of total length $\mathscr{L}$. Consider the two-conductor line shown in Fig. 5.1 where we assume for the moment resistive loads, R_S and R_L. The forward- and backward-traveling waves are related at the load, $z = \mathscr{L}$, by the *load reflection coefficient* as

$$\Gamma_L = \frac{V^-(t + \mathscr{L}/v)}{V^+(t - \mathscr{L}/v)} = \frac{R_L - Z_C}{R_L + Z_C} \tag{5.17}$$

Therefore the reflected waveform at the load can be found from the incident wave using the load reflection coefficient as

$$V^-\left(t + \frac{\mathscr{L}}{v}\right) = \Gamma_L V^+\left(t - \frac{\mathscr{L}}{v}\right) \tag{5.18}$$

The reflection coefficient so defined applies to voltage waves only. A current reflection coefficient applying to the current waves can be similarly obtained and is the negative of the voltage reflection coefficient (due to the negative sign in (5.3b)) [A.1]

$$I^-\left(t + \frac{\mathscr{L}}{v}\right) = -\Gamma_L I^+\left(t - \frac{\mathscr{L}}{v}\right) \tag{5.19}$$

The reflection at the load is illustrated in Fig. 5.2. The reflection process can be viewed as a mirror that produces, as a reflected V^-, a replica of V^+ that is "flipped around," and all points on the V^- waveform are the corresponding points on the V^+ waveform multiplied by Γ_L. Note that the total voltage at

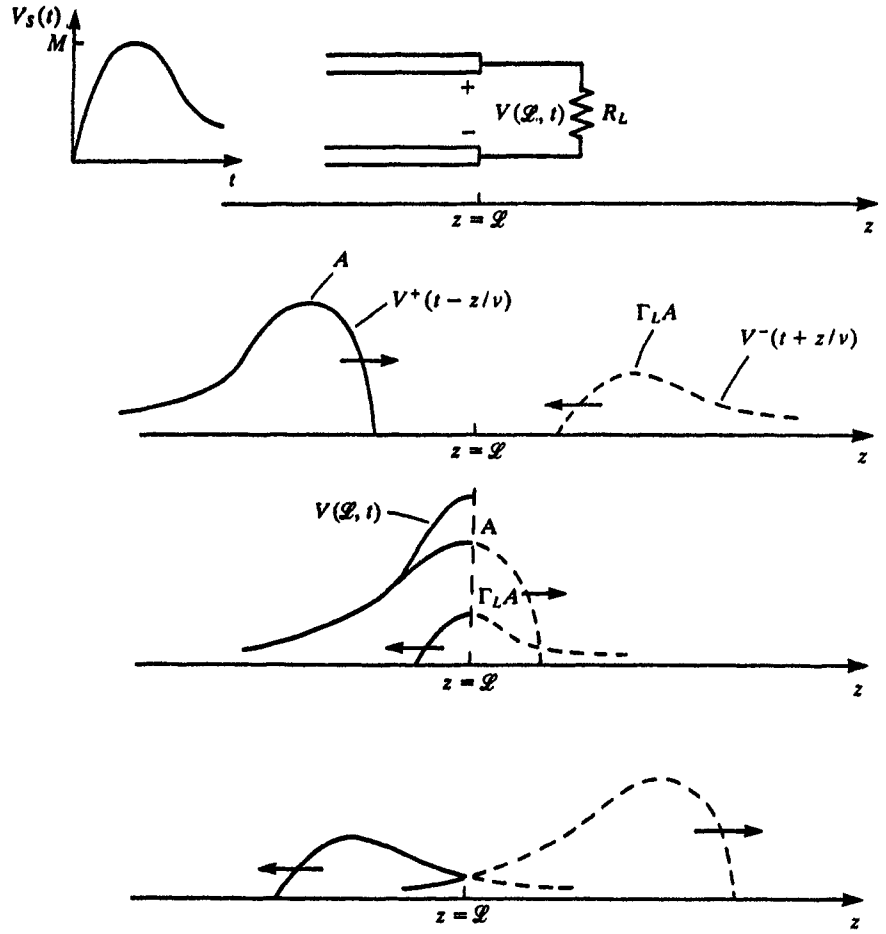

FIGURE 5.2 Illustration of reflections at a termination of a mismatched line.

the load, $V(\mathscr{L}, t)$, is the *sum* of the individual waves present at the load at a particular time as shown by (5.3a).

Now let us consider the portion of the line at the source, $z = 0$, shown in Fig. 5.3. When we initially connect the source to the line, we reason that a forward-traveling wave will be propagated down the line. We would not expect a backward-traveling wave to appear on the line until this initial forward-traveling wave has reached the load, a time delay of $T = \mathscr{L}/v$, since the incident wave will not have arrived to produce this reflected wave. The portion of the incident wave that is reflected at the load will require an additional time T to move back to the source. Therefore, for $0 \leq t \leq 2\mathscr{L}/v = 2T$, no backward-traveling waves will appear at $z = 0$, and for any time less than $2T$ the *total* voltage and current at $z = 0$ will consist only of forward-traveling waves, V^+

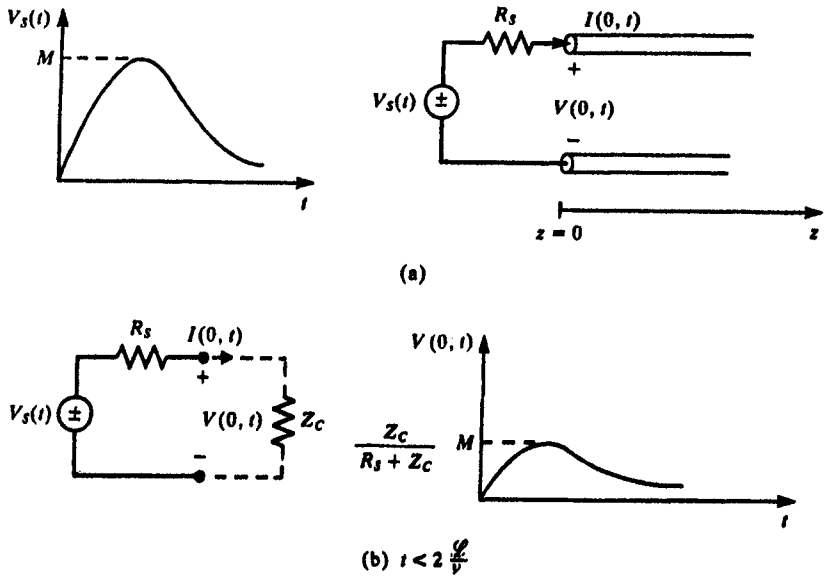

FIGURE 5.3 Characterization of the initially transmitted pulse.

and I^+. Therefore, from (5.3)

$$V(0, t) = V^+\left(t - \frac{0}{v}\right) \tag{5.20a}$$

$$I(0, t) = I^+\left(t - \frac{0}{v}\right) \tag{5.20b}$$

$$= \frac{V^+\left(t - \frac{0}{v}\right)}{Z_C} \qquad \text{for } 0 \le t \le 2T$$

Since the ratio of *total* voltage and *total* current on the line is Z_C for $0 \le t \le 2T$, the line appears to have an input resistance of Z_C over this time interval. Thus the forward-traveling voltage and current waves that are initially launched are related to the source voltage by

$$V(0, t) = \frac{Z_C}{R_S + Z_C} V_S(t) \tag{5.21a}$$

$$I(0, t) = \frac{1}{R_S + Z_C} V_S(t) \tag{5.21b}$$

This initially launched wave has the same shape as the source voltage, $V_S(t)$, (but is reversed; see Fig. 5.2).

The initially launched wave travels toward the load requiring a time $T = \mathscr{L}/v$ for the leading edge of the pulse to reach the load. When the pulse reaches the load, a reflected pulse is initiated, as shown in Fig. 5.2. This reflected pulse requires an additional time $T = \mathscr{L}/v$ for its leading edge to reach the source. At the source we can obtain a voltage reflection coefficient

$$\Gamma_S = \frac{R_S - Z_C}{R_S + Z_C} \tag{5.22}$$

as the ratio of the incoming incident wave (which is the reflected wave at the load) and the reflected portion of this incoming wave (which is sent back toward the load). A forward-traveling wave is therefore initiated at the source in the same fashion as at the load. This forward-traveling wave has the same shape as the incoming backward-traveling wave (which is the original pulse sent out by the source and reflected at the load), but corresponding points on the incoming wave are reduced by Γ_S. This process of repeated reflections continues as re-reflections at the source and the load. At any time, the total voltage (current) at any point on the line is the sum of all the individual voltage (current) waves existing on the line at that point and time, as shown by (5.3).

As an example, consider the transmission line shown in Fig. 5.4(a). At $t = 0$ a 30 V battery with zero source resistance is attached to the line, which has a total length of $\mathscr{L} = 400$ m, a velocity of propagation of $v = 200$ m/μs and a characteristic impedance of $Z_C = 50\ \Omega$. The line is terminated at the load in a $100\ \Omega$ resistor so that the load reflection coefficient is

$$\Gamma_L = \frac{100 - 50}{100 + 50}$$
$$= \tfrac{1}{3}$$

and the source reflection coefficient is

$$\Gamma_S = \frac{0 - 50}{0 + 50}$$
$$= -1$$

The one-way transit time is $T = \mathscr{L}/v = 2\mu s$. At $t = 0$ a 30 V pulse is sent down the line, and the line voltage is zero prior to the arrival of the pulse and 30 V after the pulse has passed. At $t = 2\ \mu s$ the pulse arrives at the load, and a backward-traveling pulse of magnitude $30\Gamma_L = 10$ V is sent back toward the source. When this reflected pulse arrives at the source, a pulse of magnitude Γ_S of the incoming pulse or $\Gamma_S\Gamma_L 30 = -10$ V is sent back toward the load. This

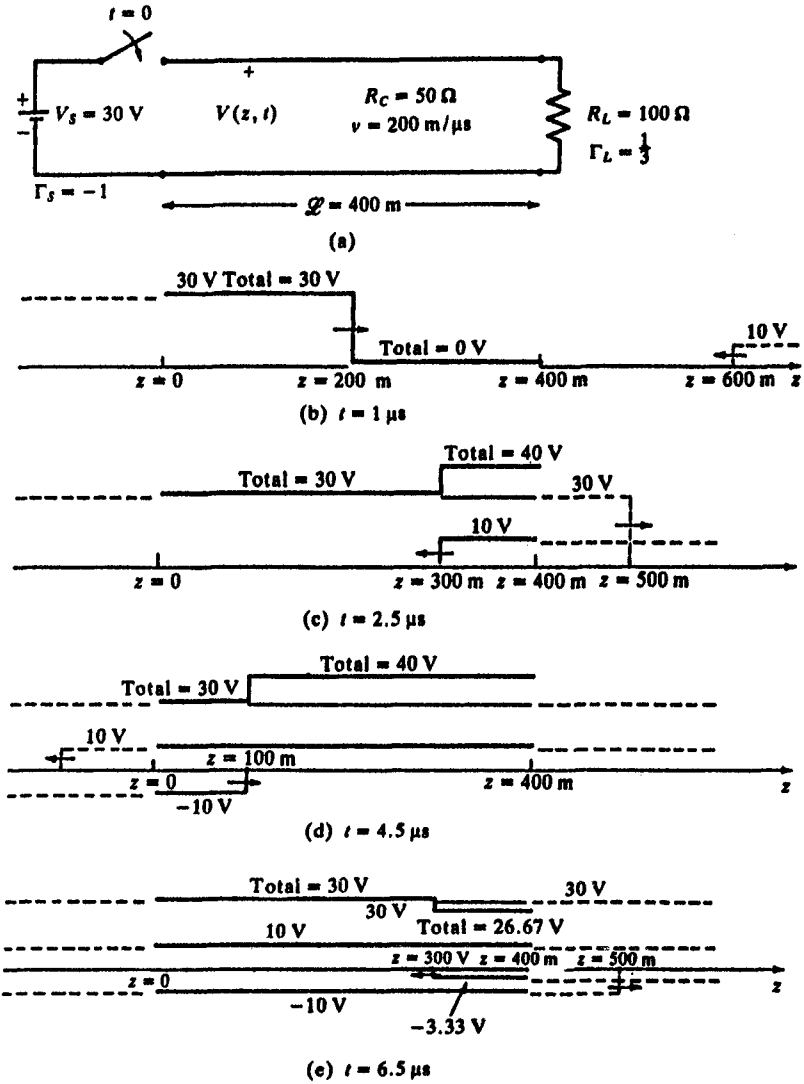

FIGURE 5.4 An example illustrating computation of the line voltage at various points on the line.

pulse travels to the load, at which time a reflected pulse of Γ_L of this incoming pulse or $\Gamma_L\Gamma_S\Gamma_L 30 = -3.33$ V is sent back toward the source. At each point on the line the total line voltage is the sum of the waves present on the line at that point.

The previous example has illustrated the process of sketching the line voltage at various points along the line and at discrete times. Generally we are only

interested in the voltage at the source and load ends of the line, $V(0, t)$ and $V(\mathscr{L}, t)$, as continuous functions of time. In order to illustrate this process, let us reconsider the previous example and sketch the voltage at the line output, $z = \mathscr{L}$, as a function of time, as illustrated in Fig. 5.5. At $t = 0$ a 30 V pulse is sent out by the source. The leading edge of this pulse arrives at the load at $t = 2$ μs. At this time a pulse of $\Gamma_L 30 = 10$ V is sent back toward the source. This 10 V pulse arrives at the source at $t = 4$ μs, and a pulse of $\Gamma_S \Gamma_L 30 = -10$ V is returned to the load. This pulse arrives at the load at $t = 6$ μs, and a pulse of $\Gamma_L \Gamma_S \Gamma_L 30 = -3.33$ V is sent back toward the source. The contributions of these waves at $z = \mathscr{L}$ are shown in Fig. 5.5(b) as dashed lines, and the total voltage is shown as a solid line. Note that the load voltage oscillates during the transient time interval about 30 V, but asymptotically converges to the expected steady-state value of 30 V. If we had attached an oscilloscope across the load to display this voltage as a function of time, and the time scale were set to 1 ms per division, it would appear that the load voltage immediately assumed a value of 30 V. We would see the picture of Fig. 5.5(b) only if the time scale of the oscilloscope were sufficiently reduced to, say, 1 μs per division. In order to sketch the load current $I(\mathscr{L}, t)$, we could divide the previously sketched load voltage by R_L. We could also sketch this directly by using current reflection coefficients $\Gamma_S = 1$ and $\Gamma_L = -\frac{1}{3}$ and an initial current pulse of $30 \text{ V}/Z_C = 0.6$ A. The current at the input to the line is sketched in this fashion in Fig. 5.5(c). Observe that the current oscillates about an expected steady-state value of $30 \text{ V}/R_L = 0.3$ A.

There are a number of other graphical methods which are equivalent to this graphical method. One of the more popular ones is referred to as the so-called lattice diagram [A.1]. This is illustrated in Fig. 5.6(a). Position along the line is plotted along the upper horizontal axis and time is plotted vertically. The initial waveform applied to the line is $Z_C/(Z_C + R_S)V_S(t)$ as shown in Fig. 5.6(b). The lattice diagram simply tracks a particular point on this applied waveform, K at t', as it travels back and forth along the line.

An *exact solution* for this general result can be obtained for any $V_S(t)$ waveform by carrying through the above graphical method to yield

$$V(0, t) = \frac{Z_C}{Z_C + R_S}\{V_S(t) + (1 + \Gamma_S)\Gamma_L V_S(t - 2T) + (1 + \Gamma_S)(\Gamma_S\Gamma_L)\Gamma_L V_S(t - 4T) + (1 + \Gamma_S)(\Gamma_S\Gamma_L)^2\Gamma_L V_S(t - 6T) + \cdots\} \tag{5.23a}$$

$$V(\mathscr{L}, t) = \frac{Z_C}{Z_C + R_S}\{(1 + \Gamma_L)V_S(t - T) + (1 + \Gamma_L)\Gamma_S\Gamma_L V_S(t - 3T) + (1 + \Gamma_L)(\Gamma_S\Gamma_L)^2 V_S(t - 5T) + (1 + \Gamma_L)(\Gamma_S\Gamma_L)^3 V_S(t - 7T) + \cdots\} \tag{5.23b}$$

This succinct form of the solution gives the time-domain voltages explicitly as

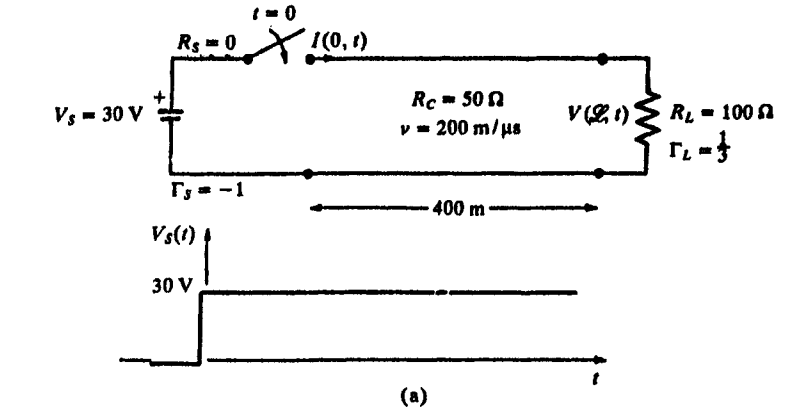

(a)

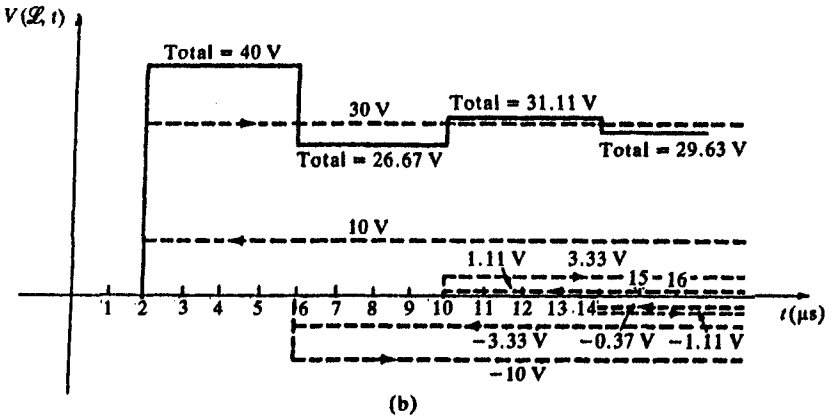

(b)

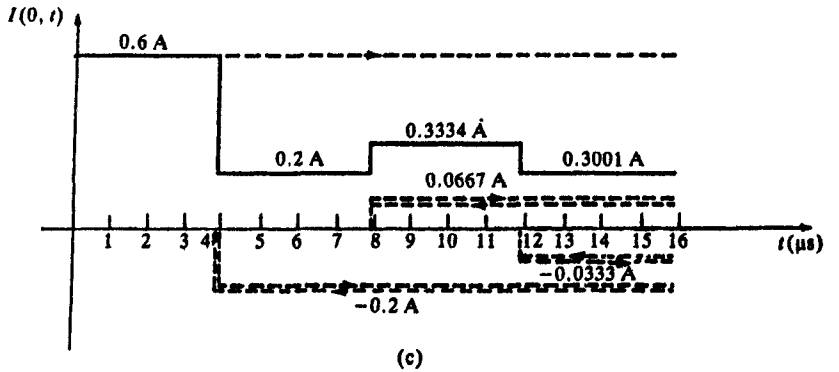

(c)

FIGURE 5.5 An example illustrating computation of the load voltage and source current as a function of time.

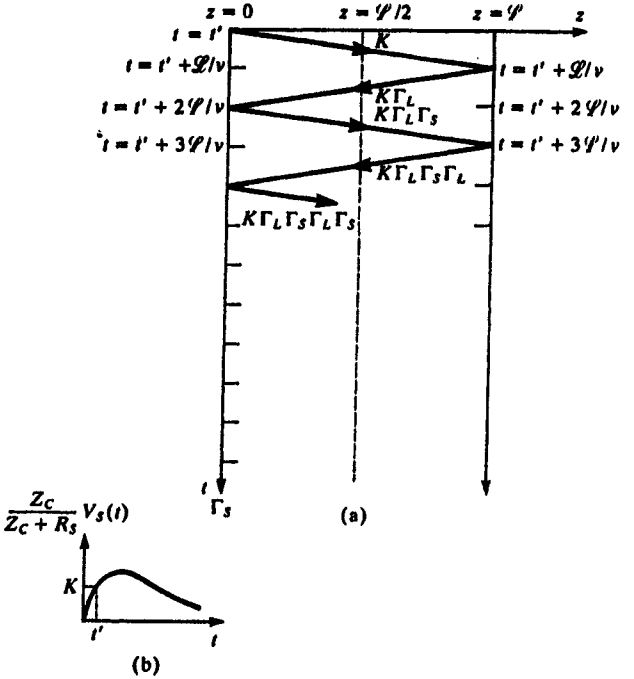

FIGURE 5.6 The lattice diagram.

scaled versions of the input signal waveform, $V_S(t)$, which are delayed by multiples of the line one-way delay, T. To compute the total solution waveforms, $V(0, t)$ and $V(\mathscr{L}, t)$, one simply draws the scaled and delayed $V_S(t)$ and adds the waveforms at corresponding time points according to (5.23).

Alternatively, this general result can be proven from an earlier frequency-domain exact solution given in (4.26a) specialized to a *lossless line*, i.e., $\hat{\gamma} = j\beta = j\omega/v$:

$$\hat{V}(z) = \frac{1 + \Gamma_L e^{-2j\omega T} e^{2j\omega z}}{1 - \Gamma_S \Gamma_L e^{-2j\omega T}} \frac{Z_C}{Z_C + R_S} \hat{V}_S e^{-j\omega z} \tag{5.24}$$

where we have substituted the one-way delay, $T = \mathscr{L}/v$. In terms of the Laplace transform variable s this becomes

$$V(0, s) = \left[\frac{1 + \Gamma_L e^{-2sT}}{1 - \Gamma_S \Gamma_L e^{-2sT}}\right] \frac{Z_C}{Z_C + R_S} V_S(s) \tag{5.25a}$$

$$V(\mathscr{L}, s) = \left[\frac{(1 + \Gamma_L) e^{-sT}}{1 - \Gamma_S \Gamma_L e^{-2sT}}\right] \frac{Z_C}{Z_C + R_S} V_S(s) \tag{5.25b}$$

Multiplying both sides by the common denominator and using (5.9) gives

$$[V(0,t) - \Gamma_S\Gamma_L V(0,t-2T)] = \frac{Z_C}{Z_C + R_S}[V_S(t) + \Gamma_L V_S(t-2T)] \quad (5.26a)$$

$$[V(\mathscr{L},t) - \Gamma_S\Gamma_L V(\mathscr{L},t-2T)] = \frac{Z_C}{Z_C + R_S}[1 + \Gamma_L]V_S(t-T) \quad (5.26b)$$

In order to examine the impact of this result we introduce the *time-shift* or *difference operator*, D, as

$$D^{\pm m}f(t) = f(t \pm mT) \quad (5.27)$$

In other words, the difference operator operates on a function of time to shift it ahead or backward in time. Substituting this result into (5.26) gives

$$[1 - \Gamma_S\Gamma_L D^{-2}]V(0,t) = \frac{Z_C}{Z_C + R_S}[1 + \Gamma_L D^{-2}]V_S(t) \quad (5.28a)$$

$$[1 - \Gamma_S\Gamma_L D^{-2}]V(\mathscr{L},t) = \frac{Z_C}{Z_C + R_S}[(1 + \Gamma_L)D^{-1}]V_S(t) \quad (5.28b)$$

Multiplying through by D^2 and rearranging into the form of a transfer function gives

$$V(0,t) = \frac{Z_C}{Z_C + R_S}\left[\frac{D^2 + \Gamma_L}{D^2 - \Gamma_S\Gamma_L}\right]V_S(t) \quad (5.29a)$$

$$= \frac{Z_C}{Z_C + R_S}[1 + (1 + \Gamma_S)\Gamma_L D^{-2} + (1 + \Gamma_S)(\Gamma_S\Gamma_L)\Gamma_L D^{-4} + (1 + \Gamma_S)(\Gamma_S\Gamma_L)^2\Gamma_L D^{-6} + \cdots]V_S(t)$$

$$V(\mathscr{L},t) = \frac{Z_C}{Z_C + R_S}\left[\frac{(1 + \Gamma_L)D}{D^2 - \Gamma_S\Gamma_L}\right]V_S(t) \quad (5.29b)$$

$$= \frac{Z_C}{Z_C + R_S}(1 + \Gamma_L)[D^{-1} + \Gamma_S\Gamma_L D^{-3} + (\Gamma_S\Gamma_L)^2 D^{-5} + \cdots]V_S(t)$$

which match the results in (5.23). Thus, for a two-conductor lossless line having resistive loads, one can immediately sketch the terminal voltage waveforms as scaled and delayed versions of the source voltage waveform, $V_S(t)$, with the result given in (5.23) or equivalently in (5.29).

5.1.2 The Method of Characteristics (Branin's Method)

The previous section has demonstrated graphical methods for sketching the time-domain solution of the transmission-line equations for linear, resistive loads. It is frequently desirable to have a numerical method that is suitable for a digital computer and will handle nonlinear as well as dynamic loads. The following method is referred to as the *method of characteristics*. The numerical implementation is attributed to Branin and was originally described in [1]. It is only valid for lossless lines.

The method of characteristics seeks to transform the partial differential equations of the transmission line into ordinary differential equations. To this end we define the *characteristic curves* in the z, t plane as

$$\frac{dz}{dt} = \frac{1}{\sqrt{lc}} \tag{5.30a}$$

$$\frac{dz}{dt} = -\frac{1}{\sqrt{lc}} \tag{5.30b}$$

The differential changes in the line voltage and current are

$$dV(z, t) = \frac{\partial V(z, t)}{\partial z} dz + \frac{\partial V(z, t)}{\partial t} dt \tag{5.31a}$$

$$dI(z, t) = \frac{\partial I(z, t)}{\partial z} dz + \frac{\partial I(z, t)}{\partial t} dt \tag{5.31b}$$

Substituting the transmission-line equations in (5.1) into (5.31) gives

$$dV(z, t) = \left(-l \frac{\partial I(z, t)}{\partial t}\right) dz + \frac{\partial V(z, t)}{\partial t} dt \tag{5.32a}$$

$$dI(z, t) = \left(-c \frac{\partial V(z, t)}{\partial t}\right) dz + \frac{\partial I(z, t)}{\partial t} dt \tag{5.32b}$$

Along the forward characteristic defined by (5.30a), $dz = 1/\sqrt{lc}\, dt$, these become

$$dV(z, t) = \left(-Z_C \frac{\partial I(z, t)}{\partial t} + \frac{\partial V(z, t)}{\partial t}\right) dt \tag{5.33a}$$

$$dI(z, t) = \left(-\frac{1}{Z_C} \frac{\partial V(z, t)}{\partial t} + \frac{\partial I(z, t)}{\partial t}\right) dt \tag{5.33b}$$

Similarly, along the backward characteristic defined by (5.30b), $dz = -1/\sqrt{lc}\, dt$,

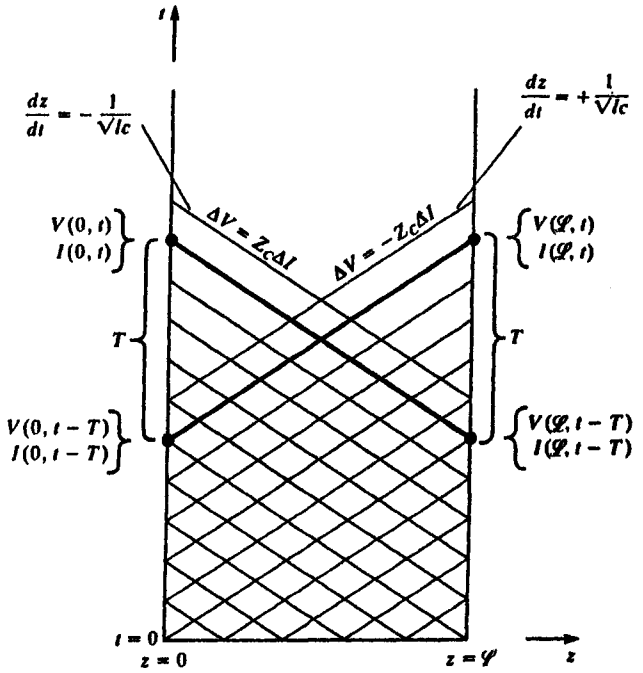

FIGURE 5.7 Illustration of characteristic curves for the method of characteristics.

these become

$$dV(z, t) = \left(Z_C \frac{\partial I(z, t)}{\partial t} + \frac{\partial V(z, t)}{\partial t}\right) dt \tag{5.34a}$$

$$dI(z, t) = \left(\frac{1}{Z_C} \frac{\partial V(z, t)}{\partial t} + \frac{\partial I(z, t)}{\partial t}\right) dt \tag{5.34b}$$

Multiplying (5.33b) by the characteristic impedance, $Z_C = \sqrt{l/c}$, and adding the equations gives

$$dV(z, t) + Z_C\, dI(z, t) = 0 \tag{5.35a}$$

Similarly, multiplying (5.34b) by the characteristic impedance, $Z_C = \sqrt{l/c}$, and subtracting the equations gives

$$dV(z, t) - Z_C\, dI(z, t) = 0 \tag{5.35b}$$

Equation (5.35a) holds along the characteristic curve defined by (5.30a) with phase velocity $v = 1/\sqrt{lc}$, while (5.35b) holds along the characteristic curve defined by (5.30b) with the same phase velocity. This is illustrated in Fig. 5.7.

These are directly integrable showing that the difference between two voltages at two points on a given characteristic is related to the difference between two currents on the same characteristic. Therefore, from Fig. 5.7 we may obtain

$$[V(\mathscr{L}, t) - V(0, t - T)] = -Z_C[I(\mathscr{L}, t) - I(0, t - T)] \tag{5.36a}$$

$$[V(0, t) - V(\mathscr{L}, t - T)] = +Z_C[I(0, t) - I(\mathscr{L}, t - T)] \tag{5.36b}$$

where the one-way delay is $T = \mathscr{L}/v$.

This result was derived earlier using the Laplace transform and given in (5.16). As an alternative derivation, we simply manipulate the solutions of the transmission-line equations given in (5.3). Rewrite these as

$$V(z, t) = V^+\left(t - \frac{z}{v}\right) + V^-\left(t + \frac{z}{v}\right) \tag{5.37a}$$

$$Z_C I(z, t) = V^+\left(t - \frac{z}{v}\right) - V^-\left(t + \frac{z}{v}\right) \tag{5.37b}$$

Evaluating these at the source end, $z = 0$, and at the load end, $z = \mathscr{L}$, gives

$$V(0, t) = V^+(t) + V^-(t) \tag{5.38a}$$

$$Z_C I(0, t) = V^+(t) - V^-(t) \tag{5.38b}$$

and

$$V(\mathscr{L}, t) = V^+(t - T) + V^-(t + T) \tag{5.39a}$$

$$Z_C I(\mathscr{L}, t) = V^+(t - T) - V^-(t + T) \tag{5.39b}$$

where the one-way delay for the line is $T = \mathscr{L}/v$. Adding and subtracting (5.38) and (5.39) gives

$$V(0, t) + Z_C I(0, t) = 2V^+(t) \tag{5.40a}$$

$$V(0, t) - Z_C I(0, t) = 2V^-(t) \tag{5.40b}$$

$$V(\mathscr{L}, t) + Z_C I(\mathscr{L}, t) = 2V^+(t - T) \tag{5.40c}$$

$$V(\mathscr{L}, t) - Z_C I(\mathscr{L}, t) = 2V^-(t + T) \tag{5.40d}$$

Shifting both (5.40a) and (5.40d) ahead in time by subtracting T from t along with a rearrangement of the equations gives

$$V(0, t) = Z_C I(0, t) + 2V^-(t) \tag{5.41a}$$

$$V(\mathscr{L}, t) = -Z_C I(\mathscr{L}, t) + 2V^+(t - T) \tag{5.41b}$$

$$V(0, t - T) + Z_C I(0, t - T) = 2V^+(t - T) \tag{5.41c}$$

$$V(\mathscr{L}, t - T) - Z_C I(\mathscr{L}, t - T) = 2V^-(t) \tag{5.41d}$$

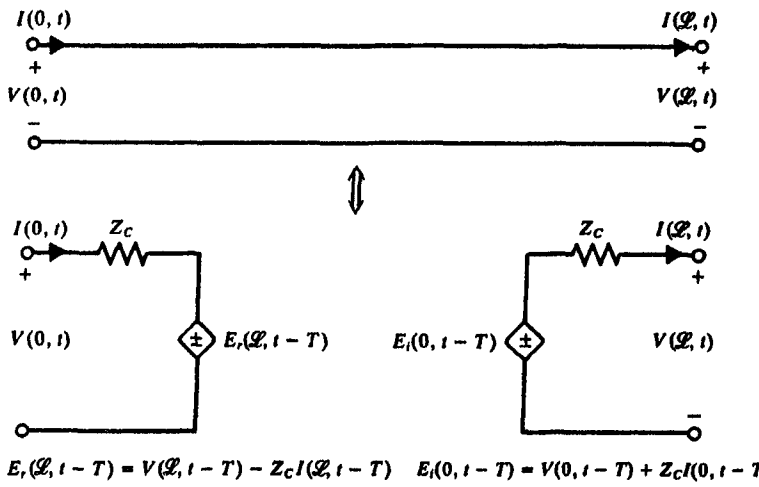

FIGURE 5.8 A time-domain equivalent circuit of a two-conductor line in terms of time-delayed controlled sources obtained from the method of characteristics (Branin's method) as implemented in SPICE.

Substituting (5.41d) into (5.41a) gives

$$V(0, t) = Z_C I(0, t) + E_r(\mathscr{L}, t - T) \tag{5.42a}$$

where

$$E_r(\mathscr{L}, t - T) = V(\mathscr{L}, t - T) - Z_C I(\mathscr{L}, t - T) \tag{5.42b}$$
$$= 2V^-(t)$$

Similarly, substituting (5.40c) into (5.40b) gives

$$V(\mathscr{L}, t) = -Z_C I(\mathscr{L}, t) + E_i(0, t - T) \tag{5.43a}$$

where

$$E_i(0, t - T) = V(0, t - T) + Z_C I(0, t - T) \tag{5.43b}$$
$$= 2V^+(t - T)$$

Equations (5.42) and (5.43) suggest the equivalent circuit of the total line shown in Fig. 5.8. The controlled source $E_i(0, t - T)$ is produced by the voltage and current at the input to the line at a time equal to a one-way transit delay earlier than the present time. Similarly, the controlled source $E_r(\mathscr{L}, t - T)$ is produced by the voltage and current at the line output at a time equal to a one-way transit delay earlier than the present time.

The equivalent circuit shown in Fig. 5.8 is an exact solution of the transmission-line equations for a lossless, two-conductor, uniform transmission line. The circuit

analysis program SPICE contains this *exact model* among its list of available circuit element models that the user may call [A.2]. The model is the TXXX element, where XXX is the model number chosen by the user. SPICE uses controlled sources having time delay to construct the equivalent circuit of Fig. 5.8. The user need only input the characteristic impedance of the line Z_C (SPICE refers to this parameter as Z0) and the one-way transit delay T (SPICE refers to this parameter as TD). Thus SPICE *will produce exact solutions of the transmission-line equations.* Furthermore, nonlinear terminations such as diodes and transistors as well as dynamic terminations such as capacitors and inductors are easily handled with the SPICE code whereas a graphical solution or the hand solution of the equivalent circuit of Fig. 5.8 for these types of loads would be quite difficult. This author highly recommends the use of SPICE for the incorporation of two-conductor transmission-line effects into any analysis of an electronic circuit. It is simple and straightforward to incorporate the transmission-line effects in any time-domain analysis of an electronic circuit, and, more importantly, models of the complicated, but typical, nonlinear loads such as diodes and transistors as well as inductors and capacitors already exist in the code and can be called on by the user rather than the user needing to develop models for these loads.

As an example of the use of SPICE to model two-conductor, lossless transmission lines in the time domain, consider the time-domain analysis of the circuit of Fig. 5.5. The 30 V source is modeled with the PWL (piecewise linear) model as transitioning from 0 V to 30 V in 0.1 μs and remaining there throughout the analysis time interval of 20 μs. The SPICE program is

```
FIGURE 5.5
VS 1 0 PWL(0 0 .1U 30 20U 30)
T 1 0 2 0 Z0 = 50 TD = 2U
RL 2 0 100
.TRAN .1U 20U
.PRINT TRAN V(2) I(VS)
.PLOT TRAN V(2) I(VS)
.END
```

The results for the load voltage are plotted using the .PROBE option of the personal computer version, PSPICE, [A.2] in Fig. 5.9(a) and the input current to the line is plotted in Fig. 5.9(b). Comparing these with the hand-calculated results shown in Fig. 5.5 shows exact agreement.

5.1.3 The Bergeron Diagram

The following graphical method was originally developed for analyzing transients in hydraulic systems by L. Bergeron in 1949 and has been adapted to transmission lines [2–4]. It can be easily proven using the equivalent circuit shown in Fig. 5.8 that was obtained from the method of characteristics. The

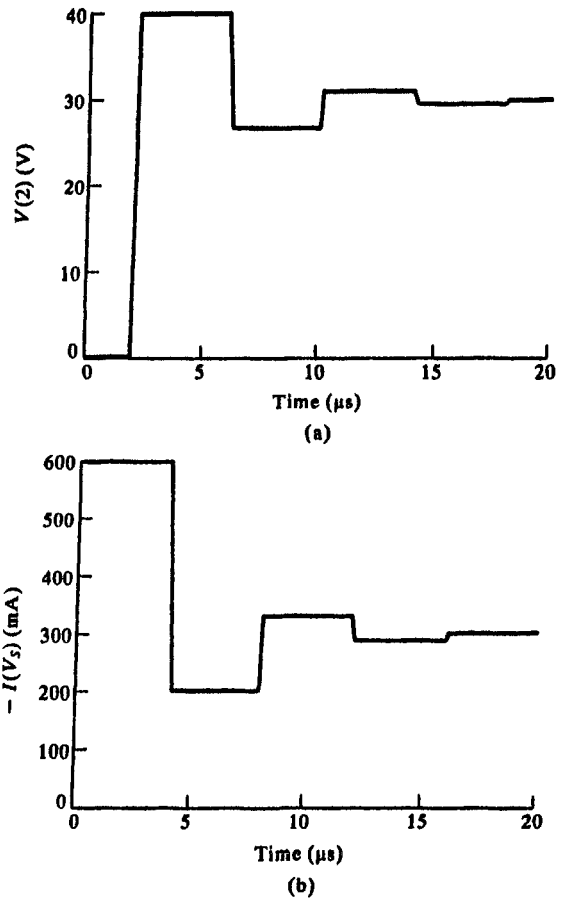

FIGURE 5.9 Results of the exact SPICE model for the problem of Fig. 5.5.

advantage of the method is that it readily handles nonlinear resistive loads on the line, such as diodes, but the disadvantage is that it is only valid for step-function excitation and resistive loads.

Consider the lossless, two-conductor line shown in Fig. 5.10(a) having resistive source and load impedances and driven by a step voltage source: $V_S(t) = V_S u(t)$. Substituting the equivalent circuit from Fig. 5.8 gives the circuit of Fig. 5.10(b). In order to simplify the notation we designate the line voltages and currents at the input and output of the line as $V(0, t) = V_{in}(t)$, $I(0, t) = I_{in}(t)$, $V(\mathscr{L}, t) = V_{out}(t)$, and $I(\mathscr{L}, t) = I_{out}(t)$. Let us choose to implement Branin's method via this equivalent circuit for *discrete times that are multiples of the one-way line delay T*. Thus we solve the circuit of Fig. 5.10(b) at $t = 0, T, 2T, 3T, \ldots$. Observe that the controlled source outputs are related to the *voltage and current at the opposite end of the line and at one time delay earlier.*

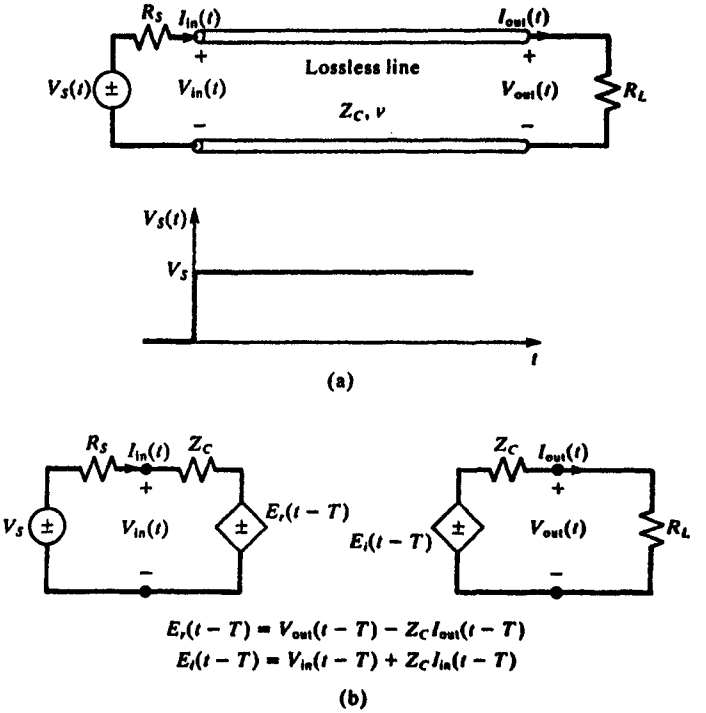

FIGURE 5.10 Illustration of the proof of the validity of the Bergeron diagram method: (a) the structure and (b) the equivalent circuit using Branin's method.

First consider the circuit at $t = 0^+$, that is immediately after $t = 0$, as shown in Fig. 5.11. The controlled source outputs depend on the line voltages and currents at $t = 0^+ - T = -T$ which are of course zero because we assume the line is initially relaxed. The solution for $V_{in}(0^+)$ and $I_{in}(0^+)$ are obtained from the simultaneous solution of the two equations written for the left circuit (at $z = 0$):

$$\text{(a)} \quad V_{in}(0^+) = Z_C I_{in}(0^+) \tag{5.44a}$$

$$\text{(b)} \quad V_{in}(0^+) = V_S - R_S I_{in}(0^+) \tag{5.44b}$$

Equation (5.44b) can be rewritten as

$$\text{(b)} \quad [V_{in}(0^+) - V_S] = -R_S I_{in}(0^+) \tag{5.44b}$$

Equations (5.44) are plotted in Fig. 5.11 and their intersection gives the solution for $V_{in}(0^+)$ and $I_{in}(0^+)$. Observe that equation (5.44a) has slope $1/Z_C$ and passes through the origin, whereas equation (5.44b) has slope $-1/R_S$ and passes through $V = V_S$.

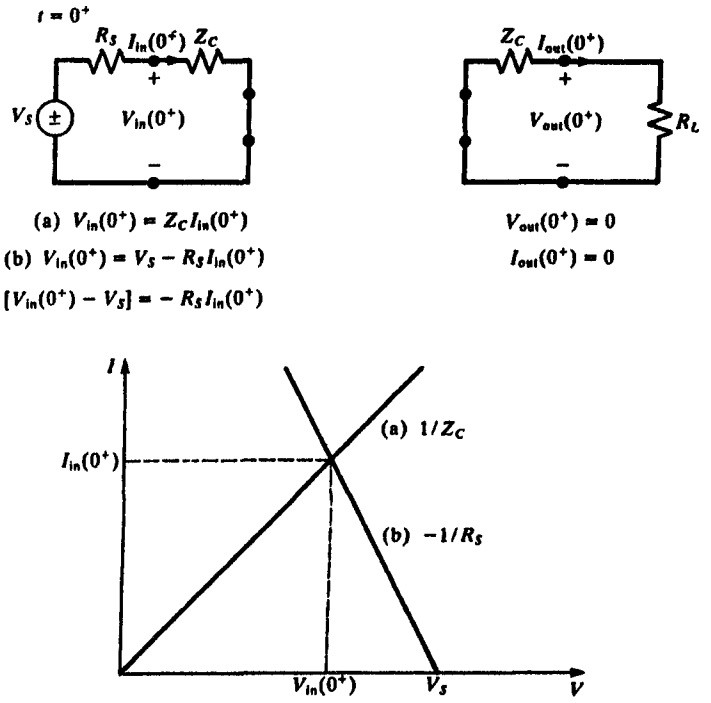

FIGURE 5.11 The Bergeron diagram at $t = 0^+$.

Next we obtain the solution at $t = T$ from the circuit of Fig. 5.12. The solutions for $V_{out}(T)$ and $I_{out}(T)$ are obtained from the simultaneous solution of the equations written for the right circuit ($z = \mathscr{L}$):

$$\text{(a)}\quad V_{out}(T) = R_L I_{out}(T) \tag{5.45a}$$

$$\text{(b)}\quad V_{out}(T) = [V_{in}(0^+) + Z_C I_{in}(0^+)] - Z_C I_{out}(T) \tag{5.45b}$$

Equation (5.45b) can be rewritten as

$$\text{(b)}\quad [V_{out}(T) - V_{in}(0^+)] = -Z_C[I_{out}(T) - I_{in}(0^+)] \tag{5.45b}$$

Equations (5.46) are plotted in Fig. 5.12 and their intersection gives the solutions for $V_{out}(T)$ and $I_{out}(T)$. Observe that equation (5.45a) has slope $1/R_L$ and passes through the origin, whereas equation (5.45b) has slope $-1/Z_C$ and passes through the first solution point. Thus the solution proceeds along line (b).

Next we obtain the solution at $t = 2T$ from the circuit of Fig. 5.13. The solutions for $V_{in}(2T)$ and $I_{in}(2T)$ are obtained from the simultaneous solution

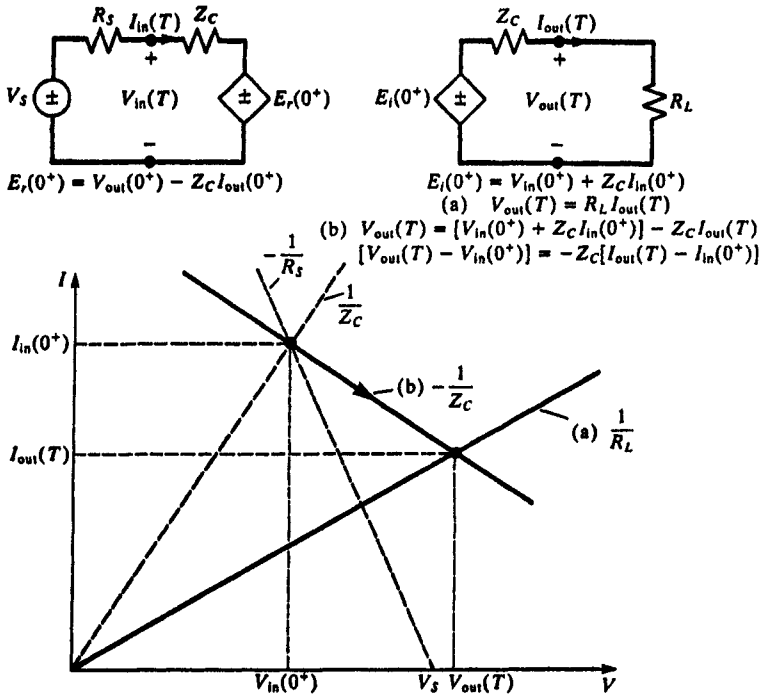

FIGURE 5.12 The Bergeron diagram at $t = T$.

of the equations written for the left circuit ($z = 0$):

$$\text{(a)}\quad V_{in}(2T) = V_S - R_S I_{in}(2T) \tag{5.46a}$$

$$\text{(b)}\quad V_{in}(2T) = [V_{out}(T) - Z_C I_{out}(T)] + Z_C I_{in}(2T) \tag{5.46b}$$

Equations (5.46) can be rewritten as

$$\text{(a)}\quad [V_{in}(2T) - V_S] = -R_S I_{in}(2T) \tag{5.46a}$$

$$\text{(b)}\quad [V_{in}(2T) - V_{out}(T)] = Z_C[I_{in}(2T) - I_{out}(T)] \tag{5.46b}$$

Equations (5.46) are plotted in Fig. 5.13 and their intersection gives the solutions for $V_{in}(2T)$ and $I_{in}(2T)$. Observe that equation (5.46a) has slope $-1/R_S$ and passes through $V = V_S$, whereas equation (5.46b) has slope $1/Z_C$ and passes through the second solution point. Thus the solution proceeds along line (b).

The solution continues in like fashion by alternating between the left and right circuits at time increments of T. This produces the time-domain solution valid at each end at times separated by $2T$ as shown in Fig. 5.14. The value of

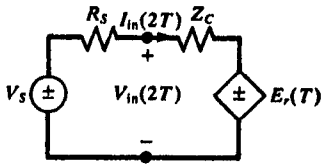

$$E_r(T) = V_{out}(T) - Z_C I_{out}(T) \qquad E_i(T) = V_{in}(T) + Z_C I_{in}(T)$$

(a) $V_{in}(2T) = V_S - R_S I_{in}(2T)$

$[V_{in}(2T) - V_S] = -R_S I_{in}(2T)$

(b) $V_{in}(2T) = [V_{out}(T) - Z_C I_{out}(T)] + Z_C I_{in}(2T)$

$[V_{in}(2T) - V_{out}(T)] = Z_C [I_{in}(2T) - I_{out}(T)]$

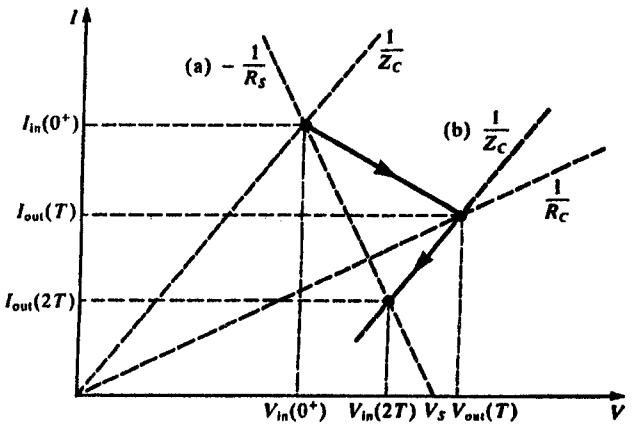

FIGURE 5.13 The Bergeron diagram at $t = 2T$.

this method lies in its ability to handle nonlinear resistive loads such as diodes as illustrated in Fig. 5.15. Numerous electronic design manuals use this method for these purposes.

5.2 MULTICONDUCTOR LOSSLESS LINES

In this section we examine the time-domain solution of the MTL equations for a *lossless line*:

$$\frac{\partial}{\partial z}\mathbf{V}(z, t) = -\mathbf{L}\frac{\partial}{\partial t}\mathbf{I}(z, t) \tag{5.47a}$$

$$\frac{\partial}{\partial z}\mathbf{I}(z, t) = -\mathbf{C}\frac{\partial}{\partial t}\mathbf{V}(z, t) \tag{5.47b}$$

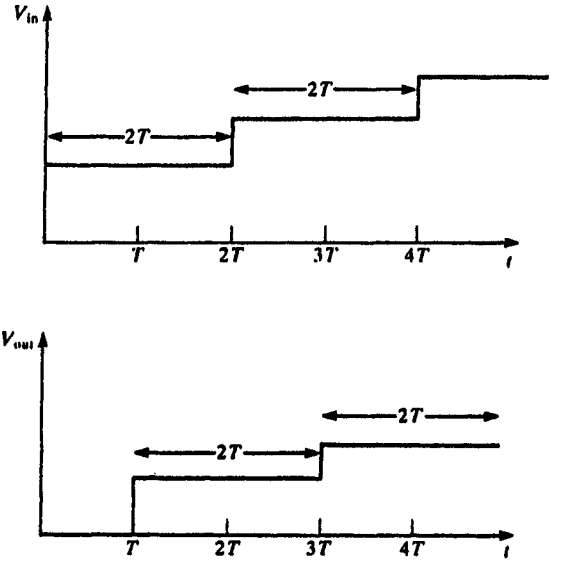

FIGURE 5.14 Illustration of the line input and output voltages computed via the Bergeron diagram.

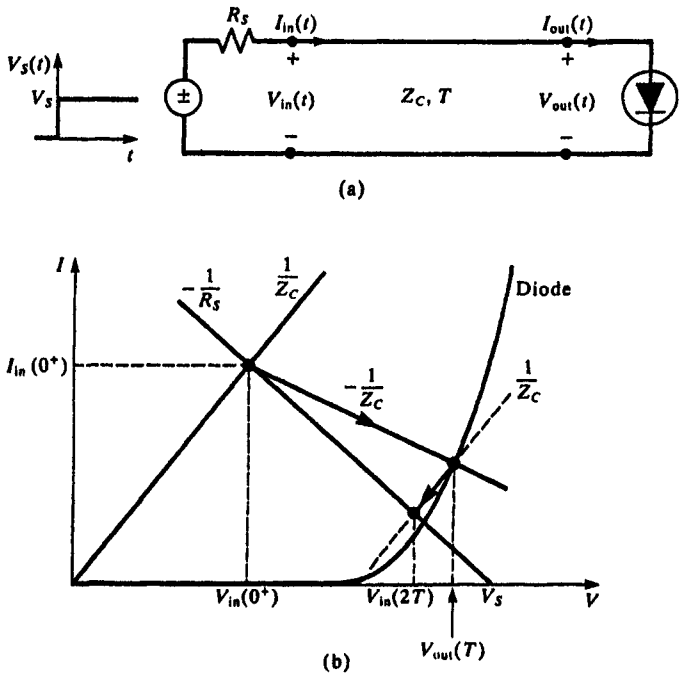

FIGURE 5.15 Use of the Bergeron diagram to compute time-domain responses of the line for nonlinear, resistive loads.

The uncoupled, second-order equations are

$$\frac{\partial^2}{\partial z^2}\mathbf{V}(z,t) = \mathbf{LC}\frac{\partial^2}{\partial t^2}\mathbf{V}(z,t) \tag{5.48a}$$

$$\frac{\partial^2}{\partial z^2}\mathbf{I}(z,t) = \mathbf{CL}\frac{\partial^2}{\partial t^2}\mathbf{I}(z,t) \tag{5.48b}$$

Note that the order of multiplication of **L** and **C** in the second-order equations in (5.48) must be strictly observed. The objective in this section is to determine the general solution of these equations *and* the incorporation of the terminal conditions.

5.2.1 Decoupling the MTL Equations

The primary technique used to determine the general form of the solution of the MTL equations for *sinusoidal, steady-state excitation* in the previous chapter was to *decouple them with a similarity transformation.* In the case of the general time-domain solution of *lossless lines,* the technique of decoupling the MTL equations in (5.47) or (5.48) via a similarity transformation is again a useful technique that can always be used to find the solution.

As in the previous chapter we define the similarity transformations to *mode voltages* and *currents* as:

$$\mathbf{V}(z,t) = \mathbf{T}_V\mathbf{V}_m(z,t) \tag{5.49a}$$

$$\mathbf{I}(z,t) = \mathbf{T}_I\mathbf{I}_m(z,t) \tag{5.49b}$$

Substituting these into (5.47) give

$$\frac{\partial}{\partial z}\mathbf{V}_m(z,t) = -\mathbf{T}_V^{-1}\mathbf{L}\mathbf{T}_I\frac{\partial}{\partial t}\mathbf{I}_m(z,t) \tag{5.50a}$$

$$\frac{\partial}{\partial z}\mathbf{I}_m(z,t) = -\mathbf{T}_I^{-1}\mathbf{C}\mathbf{T}_V\frac{\partial}{\partial t}\mathbf{V}_m(z,t) \tag{5.50b}$$

or for the uncoupled second-order equations in (5.48)

$$\frac{\partial^2}{\partial z^2}\mathbf{V}_m(z,t) = \mathbf{T}_V^{-1}\mathbf{L}\mathbf{C}\mathbf{T}_V\frac{\partial^2}{\partial t^2}\mathbf{V}_m(z,t) \tag{5.51a}$$

$$\frac{\partial^2}{\partial z^2}\mathbf{I}_m(z,t) = \mathbf{T}_I^{-1}\mathbf{C}\mathbf{L}\mathbf{T}_I\frac{\partial^2}{\partial t^2}\mathbf{I}_m(z,t) \tag{5.51b}$$

If we can choose a $\mathbf{T}_V$ and a $\mathbf{T}_I$ such that (5.50) or (5.51) are uncoupled then

we have the general form of the mode solutions as those of two-conductor lines of the previous section. This is always guaranteed for *lossless lines* as was shown in the previous chapter for sinusoidal excitation. For example, consider the coupled first-order equations in (5.50). Suppose we can find a $\mathbf{T}_V$ and a $\mathbf{T}_I$ such that they simultaneously diagonalize both $\mathbf{L}$ and $\mathbf{C}$ as

$$\mathbf{T}_V^{-1}\mathbf{L}\mathbf{T}_I = \mathbf{L}_m \tag{5.52a}$$

$$\mathbf{T}_I^{-1}\mathbf{C}\mathbf{T}_V = \mathbf{C}_m \tag{5.52b}$$

where $\mathbf{L}_m$ and $\mathbf{C}_m$ are *diagonal* as

$$\mathbf{L}_m = \begin{bmatrix} l_{m1} & 0 & \cdots & 0 \\ 0 & l_{m2} & \ddots & \vdots \\ \vdots & \ddots & \ddots & 0 \\ 0 & \cdots & 0 & l_{mn} \end{bmatrix} \tag{5.52c}$$

$$\mathbf{C}_m = \begin{bmatrix} c_{m1} & 0 & \cdots & 0 \\ 0 & c_{m2} & \ddots & \vdots \\ \vdots & \ddots & \ddots & 0 \\ 0 & \cdots & 0 & c_{mn} \end{bmatrix} \tag{5.52d}$$

Then the mode equations in (5.50) become

$$\frac{\partial}{\partial z}\mathbf{V}_m(z,t) = -\mathbf{L}_m \frac{\partial}{\partial t}\mathbf{I}_m(z,t) \tag{5.53a}$$

$$\frac{\partial}{\partial z}\mathbf{I}_m(z,t) = -\mathbf{C}_m \frac{\partial}{\partial t}\mathbf{V}_m(z,t) \tag{5.53b}$$

or

$$\left.\begin{aligned} \frac{\partial}{\partial z}V_{m1}(z,t) &= -l_{m1}\frac{\partial}{\partial t}I_{m1}(z,t) \\ \frac{\partial}{\partial z}I_{m1}(z,t) &= -c_{m1}\frac{\partial}{\partial t}V_{m1}(z,t) \\ &\vdots \\ \frac{\partial}{\partial z}V_{mn}(z,t) &= -l_{mn}\frac{\partial}{\partial t}I_{mn}(z,t) \\ \frac{\partial}{\partial z}I_{mn}(z,t) &= -c_{mn}\frac{\partial}{\partial t}V_{mn}(z,t) \end{aligned}\right\} \tag{5.54}$$

These are the same equations as for *uncoupled, two-conductor lines* having characteristic impedances of

$$Z_{Cmi} = \sqrt{\frac{l_{mi}}{c_{mi}}} \tag{5.55}$$

and velocities of propagation of

$$v_{mi} = \frac{1}{\sqrt{l_{mi} c_{mi}}} \tag{5.56}$$

Therefore the solutions for these mode voltages and currents have the same general form as for the two-conductor line. The actual voltages and currents can be obtained from the forms of the mode voltage and current solutions via (5.49). We now address the determination of the diagonalizing similarity transformation for several classes of lines.

5.2.1.1 Lossless Lines in Homogeneous Media For this class of line we have the important identity

$$\mathbf{LC} = \mathbf{CL} = \mu\varepsilon \mathbf{1}_n \tag{5.57}$$

where the surrounding *homogeneous* medium is characterized by permittivity, ε, and permeability, μ. The similarity transformations that simultaneously diagonalize L and C as in (5.52) can be found in the following manner as shown in the previous chapter. Because L is real symmetric, a real *orthogonal* transformation T can be found such that

$$\mathbf{T}^t \mathbf{L} \mathbf{T} = \mathbf{L}_m \tag{5.58a}$$

where

$$\mathbf{L}_m = \begin{bmatrix} l_{m1} & 0 & \cdots & 0 \\ 0 & l_{m1} & \ddots & \vdots \\ \vdots & \ddots & \ddots & 0 \\ 0 & \cdots & 0 & l_{m1} \end{bmatrix} \tag{5.58b}$$

and the inverse of T is its transpose [5]:

$$\mathbf{T}^{-1} = \mathbf{T}^t \tag{5.58c}$$

Similarly, with the aid of the identity in (5.57) expressed as

$$\mathbf{C} = \mu\varepsilon \mathbf{L}^{-1} \tag{5.59}$$

we may form

$$\mathbf{T}^{-1}\mathbf{C}(\mathbf{T}^t)^{-1} = \mathbf{T}^t\mathbf{C}\mathbf{T} \tag{5.60}$$
$$= \mu\varepsilon\mathbf{T}^t\mathbf{L}^{-1}\mathbf{T}$$
$$= \frac{1}{v^2}\mathbf{L}_m^{-1}$$

Comparing (5.58) and (5.60) to (5.52) shows that the transformations can be defined as

$$\mathbf{T}_I = \mathbf{T} \tag{5.61a}$$

$$\mathbf{T}_V = \mathbf{T} \tag{5.61b}$$

$$\mathbf{T}_I^{-1} = \mathbf{T}_V^{-1} = \mathbf{T}^t \tag{5.61c}$$

Therefore the mode characteristic impedances in (5.55) are

$$Z_{Cmi} = vl_{mi} \tag{5.62}$$

and all modes have the same velocity of propagation:

$$v_{mi} = \frac{1}{\sqrt{\mu\varepsilon}} \tag{5.63}$$

For the special case of a three-conductor line, $n = 2$, the mode transformation is simple:

$$\mathbf{T} = \begin{bmatrix} \cos\theta & -\sin\theta \\ \sin\theta & \cos\theta \end{bmatrix} \tag{5.64a}$$

where

$$\tan 2\theta = \frac{2l_{12}}{l_{11} - l_{22}} \tag{5.64b}$$

For $n \geq 3$ a numerical computer subroutine implementing, for example, the Jacobi method must be used to obtain the orthogonal transformation [5]. Appendix A describes a FORTRAN subroutine, **JACOBI.SUB** supplied with this text which accomplishes this reduction.

5.2.1.2 Lossless Lines in Inhomogeneous Media For this we no longer have the identity in (5.57). However, we showed in Chapter 4 that because **L** and **C** are real, symmetric, and positive definite we can find a transformation that simultaneously diagonalizes these matrices in the following manner. First we find an orthogonal transformation that diagonalizes **C** as

$$\mathbf{U}^t\mathbf{C}\mathbf{U} = \boldsymbol{\theta}^2 \tag{5.65a}$$

where

$$\boldsymbol{\theta}^2 = \begin{bmatrix} \theta_1^2 & 0 & \cdots & 0 \\ 0 & \theta_2^2 & \ddots & \vdots \\ \vdots & \ddots & \ddots & 0 \\ 0 & \cdots & 0 & \theta_n^2 \end{bmatrix} \tag{5.65b}$$

and

$$\mathbf{U}^{-1} = \mathbf{U}^t \tag{5.65c}$$

Since **C** is positive definite, we can obtain its square root, $\boldsymbol{\theta}$, which is real and nonsingular and form the product $\boldsymbol{\theta}\mathbf{U}^t\mathbf{L}\mathbf{U}\boldsymbol{\theta}$. Since this is real and symmetric, we can diagonalize it with another orthogonal transformation as

$$\mathbf{S}^t(\boldsymbol{\theta}\mathbf{U}^t\mathbf{L}\mathbf{U}\boldsymbol{\theta})\mathbf{S} = \boldsymbol{\Lambda}^2 \tag{5.66a}$$

where

$$\boldsymbol{\Lambda}^2 = \begin{bmatrix} \Lambda_1^2 & 0 & \cdots & 0 \\ 0 & \Lambda_2^2 & \ddots & \vdots \\ \vdots & \ddots & \ddots & 0 \\ 0 & \cdots & 0 & \Lambda_n^2 \end{bmatrix} \tag{5.66b}$$

and

$$\mathbf{S}^{-1} = \mathbf{S}^t \tag{5.66c}$$

Define the matrix **T** as

$$\mathbf{T} = \mathbf{U}\boldsymbol{\theta}\mathbf{S} \tag{5.67}$$

The columns of **T** can be normalized to a Euclidean length of unity as

$$\mathbf{T}_{\text{norm}} = \mathbf{T}\boldsymbol{\alpha} \tag{5.68}$$

where $\boldsymbol{\alpha}$ is the $n \times n$ diagonal matrix with entries

$$\alpha_{ii} = \frac{1}{\sqrt{\sum_{k=1}^{n} T_{ki}^2}} \tag{5.69a}$$

$$\alpha_{ij} = 0 \tag{5.69b}$$

The mode transformations in (5.49) that simultaneously diagonalize **L** and **C**

as in (5.52) can then be defined as

$$\mathbf{T}_I = \mathbf{U}\theta\mathbf{S}\alpha \tag{5.70a}$$

$$= \mathbf{T}_{\text{norm}}$$

$$\mathbf{T}_V = \mathbf{U}\theta^{-1}\mathbf{S}\alpha^{-1} \tag{5.70b}$$

$$= (\mathbf{T}_{\text{norm}}^t)^{-1}$$

Also

$$\mathbf{T}_I^{-1} = \alpha^{-1}\mathbf{S}^t\theta^{-1}\mathbf{U}^t \tag{5.71a}$$

$$= \mathbf{T}_V^t$$

$$\mathbf{T}_V^{-1} = \alpha\mathbf{S}^t\theta\mathbf{U}^t \tag{5.71b}$$

$$= \mathbf{T}_I^t$$

Substituting (5.70) and (5.71) into (5.52) gives

$$\mathbf{T}_V^{-1}\mathbf{L}\mathbf{T}_I = \alpha\mathbf{S}^t\theta\mathbf{U}^t\mathbf{L}\mathbf{U}\theta\mathbf{S}\alpha \tag{5.72a}$$

$$= \alpha\Lambda^2\alpha$$

$$\mathbf{T}_I^{-1}\mathbf{C}\mathbf{T}_V = \alpha^{-1}\mathbf{S}^t\theta^{-1}\mathbf{U}^t\mathbf{C}\mathbf{U}\theta^{-1}\mathbf{S}\alpha^{-1} \tag{5.72b}$$

$$= \alpha^{-2}$$

Comparing (5.72) and (5.52) shows that

$$\mathbf{L}_m = \alpha\Lambda^2\alpha \tag{5.73a}$$

$$\mathbf{C}_m = \alpha^{-2} \tag{5.73b}$$

Since α and Λ are diagonal matrices, the mode characteristic impedances and velocities of propagation are given by

$$Z_{Cml} = \sqrt{\frac{l_{ml}}{c_{ml}}} \tag{5.74}$$

$$= \alpha_{ll}^2\Lambda_l$$

and

$$v_{ml} = \frac{1}{\sqrt{l_{ml}c_{ml}}} \tag{5.75}$$

$$= \frac{1}{\Lambda_l}$$

One can show that $\mathbf{Z}_C = (\mathbf{T}_I^t)^{-1}\mathbf{Z}_{Cm}\mathbf{T}_I^{-1}$. The desired mode transformation

matrices are

$$\mathbf{T}_V = \mathbf{U}\boldsymbol{\theta}^{-1}\mathbf{S}\boldsymbol{\alpha}^{-1} \tag{5.76a}$$

$$= (\mathbf{T}'_{\text{norm}})^{-1}$$

$$\mathbf{T}_I^{-1} = \boldsymbol{\alpha}^{-1}\mathbf{S}'\boldsymbol{\theta}^{-1}\mathbf{U}' \tag{5.76b}$$

$$= \mathbf{T}_{\text{norm}}^{-1}$$

The above diagonalization is implemented in the digital computer FORTRAN subroutine **DIAG.SUB** described in Appendix A. This subroutine calls the FORTRAN subroutine **JACOBI.SUB** to compute the two orthogonal transformations required by **DIAG.SUB**.

5.2.1.3 Incorporating the Terminal Conditions via the SPICE Program Since we have uncoupled the equations via the mode transformation in the preceding sections, the mode voltages and currents are essentially associated with n *uncoupled two-conductor transmission lines* as is illustrated in (5.54) whose general solutions are known. Again each general mode solution contains two undetermined constants so that there are a total of $2n$ undetermined constants. It remains to incorporate the terminal conditions at the two ends of the line in order to evaluate these $2n$ undetermined constants.

There are a number of ways of doing this. The simplest and most useful way is to utilize the exact time-domain model that exists in the SPICE code as shown in Fig. 5.8 [A.2, A.3, 10]. But each of these models only relates the n mode voltages and currents at the two ends of the line. In order to relate these mode quantities to the actual voltages and currents we implement the mode transformations given in (5.49). These transformations can be implemented in the SPICE program through the use of controlled sources as illustrated in Fig. 5.16. Writing out the transformations in (5.49) gives

$$\begin{bmatrix} V_1(z,t) \\ V_2(z,t) \\ \vdots \\ V_n(z,t) \end{bmatrix} = \begin{bmatrix} T_{V11} & T_{V12} & \cdots & T_{V1n} \\ T_{V21} & T_{V22} & \ddots & \vdots \\ \vdots & \ddots & \ddots & \vdots \\ T_{Vn1} & \cdots & \cdots & T_{Vnn} \end{bmatrix} \begin{bmatrix} V_{m1}(z,t) \\ V_{m2}(z,t) \\ \vdots \\ V_{mn}(z,t) \end{bmatrix} \tag{5.77a}$$

$$\begin{bmatrix} I_1(z,t) \\ I_2(z,t) \\ \vdots \\ I_n(z,t) \end{bmatrix} = \begin{bmatrix} T_{I11} & T_{I12} & \cdots & T_{I1n} \\ T_{I21} & T_{I22} & \ddots & \vdots \\ \vdots & \ddots & \ddots & \vdots \\ T_{In1} & \cdots & \cdots & T_{Inn} \end{bmatrix} \begin{bmatrix} I_{m1}(z,t) \\ I_{m2}(z,t) \\ \vdots \\ I_{mn}(z,t) \end{bmatrix} \tag{5.77b}$$

where we denote the entries in $\mathbf{T}_V$ and $\mathbf{T}_I$ as T_{Vij} and T_{Iij}, respectively. Inverting

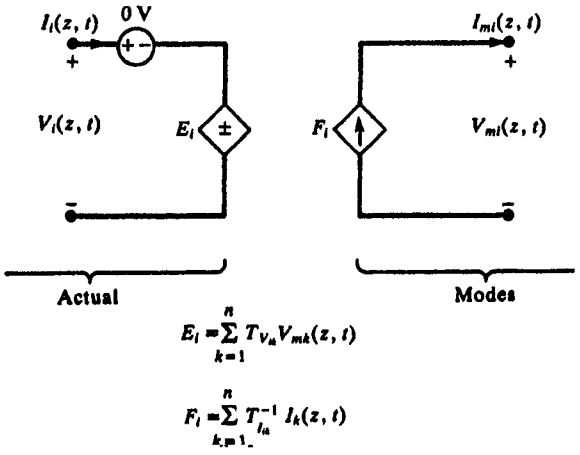

FIGURE 5.16 Illustration of the implementation of the mode transformations using controlled sources.

(5.77b) gives

$$\begin{bmatrix} I_{m1}(z,t) \\ I_{m2}(z,t) \\ \vdots \\ I_{mn}(z,t) \end{bmatrix} = \begin{bmatrix} T_{I11}^{-1} & T_{I12}^{-1} & \cdots & T_{I1n}^{-1} \\ T_{I21}^{-1} & T_{I22}^{-1} & \ddots & \vdots \\ \vdots & \ddots & \ddots & \vdots \\ T_{In1}^{-1} & \cdots & \cdots & T_{Inn}^{-1} \end{bmatrix} \begin{bmatrix} I_1(z,t) \\ I_2(z,t) \\ \vdots \\ I_n(z,t) \end{bmatrix} \tag{5.77c}$$

where we denote the entries in $\mathbf{T}_I^{-1}$ as T_{Iij}^{-1}. The transformations in (5.77a) and (5.77c) can be implemented in SPICE using the controlled source representation illustrated in Fig. 5.16. Zero-volt voltage sources are placed in each input to sample the current $I_i(z,t)$ for use in the controlled sources representing the transformation in (5.77c). The interior two-conductor mode lines having characteristic impedance Z_{Cmi} and time delay $T_i = \mathscr{L}/v_{mi}$ are simulated with the existing two-conductor SPICE model as

```
TXXX i1 i2 Z0 = ZCmi TD=Ti
```

as shown in Fig. 5.17.

The advantages of this method of implementing the terminal conditions is that the model for the line is independent of the terminations, and any of the available device models in SPICE such as resistors, capacitors, inductors as well as the nonlinear models such as diodes and transistors can be called. The user need not redevelop the mathematical models of those devices. The overall model of the line can be implemented as a subcircuit model in SPICE and the

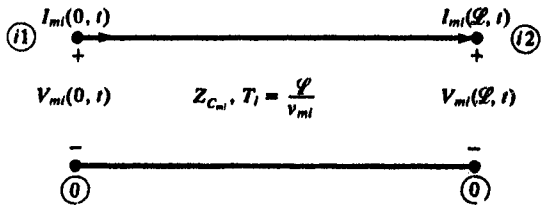

FIGURE 5.17 Characterization of the uncoupled modes as two-conductor lines with Branin's method.

appropriate line terminations attached to the ports of this subcircuit. Thus the solution is an *exact* one within the time-step discretization in the SPICE solution.

As an example of the implementation of this valuable technique, consider the example of three rectangular-cross-section conductors (lands) on the surface of a printed circuit board (PCB) shown in Fig. 5.18 that has been considered previously. This problem is that of an inhomogeneous medium and we shall assume a lossless medium and lossless conductors so that the results of Section 5.2.1.2 will apply. The per-unit-length capacitance matrix was computed using the numerical technique described in Chapter 3 via the **PCBGAL.FOR** program discussed in Appendix B:

$$\mathbf{C} = \begin{bmatrix} 40.6280 & -20.3140 \\ -20.3140 & 29.7632 \end{bmatrix} \text{pF/m}$$

The per-unit-length inductance matrix was computed from the capacitance matrix with the dielectric board removed, $\mathbf{C}_o$, as

$$\begin{aligned} \mathbf{L} &= \mu_o \varepsilon_o \mathbf{C}_o^{-1} \\ &= \begin{bmatrix} 1.10418 & 0.690094 \\ 0.690094 & 1.38019 \end{bmatrix} \mu\text{H/m} \end{aligned}$$

The similarity transformations become

$$\mathbf{T}_V = \begin{bmatrix} 1.118 & 0.5 \\ -1.234 \times 10^{-5} & 1.0 \end{bmatrix}$$

and

$$\mathbf{T}_I^{-1} = \mathbf{T}_V^t = \begin{bmatrix} 1.118 & -1.234 \times 10^{-5} \\ 0.5 & 1.0 \end{bmatrix}$$

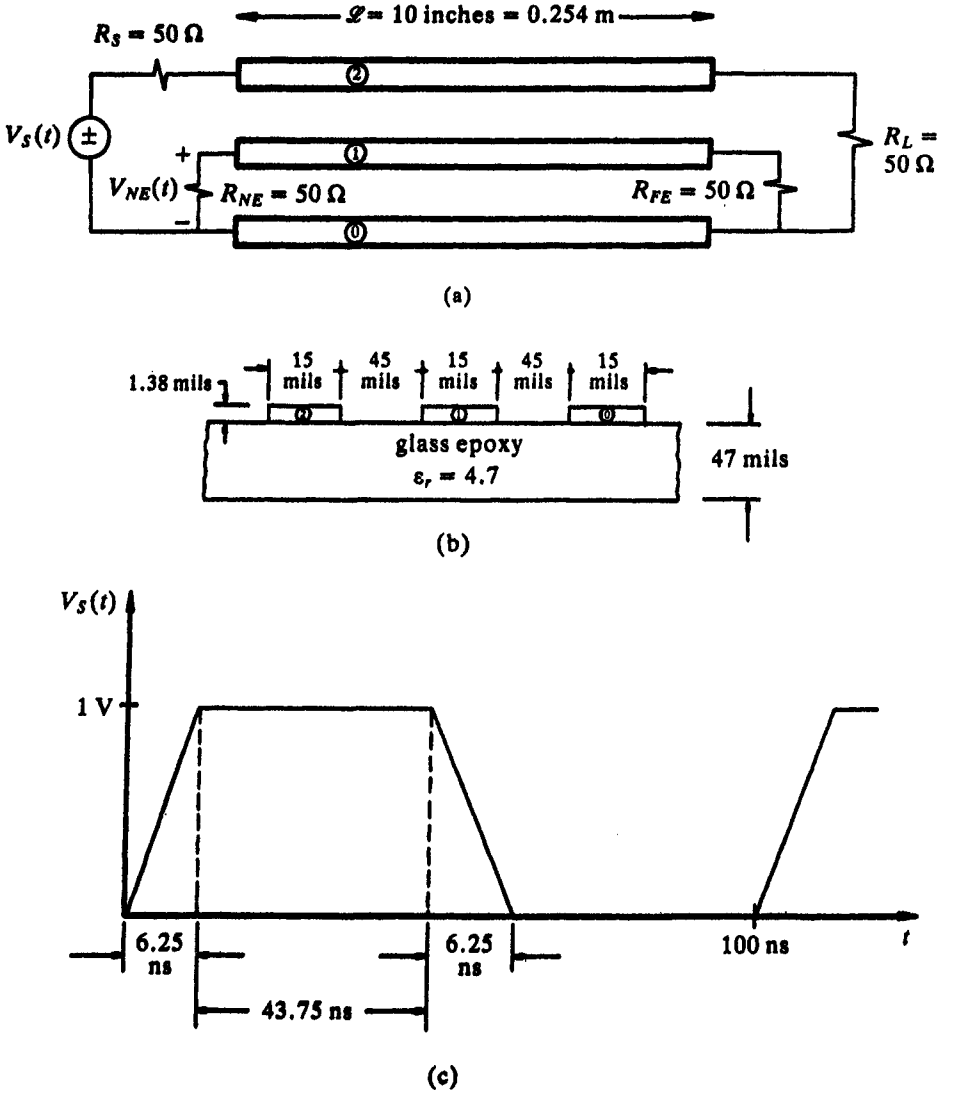

FIGURE 5.18 An example to illustrate the modeling of a MTL via Branin's method.

The mode characteristic impedances and propagation velocities are

$$Z_{Cm1} = 109.354\ \Omega$$
$$v_{m1} = 1.800\,65 \times 10^8\ \text{m/s}$$
$$Z_{Cm2} = 265.325\ \Omega$$
$$v_{m2} = 1.922\,36 \times 10^8\ \text{m/s}$$

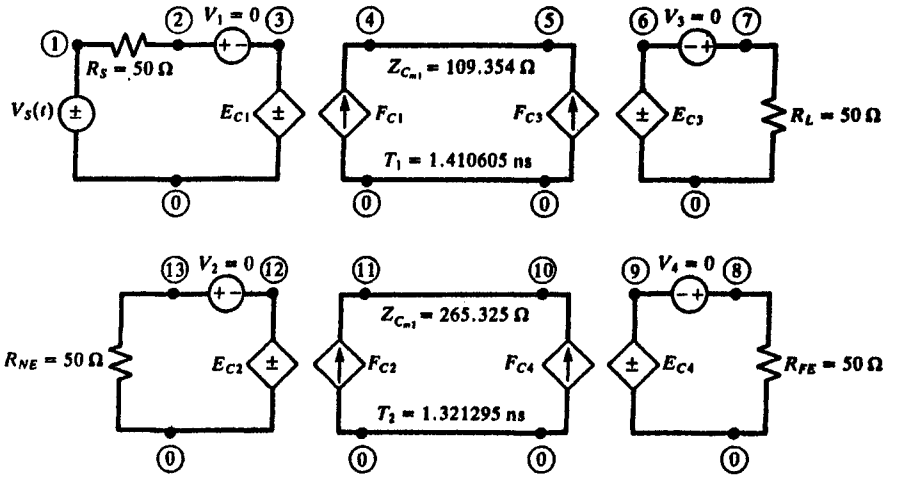

FIGURE 5.19 The SPICE equivalent circuit for the structure of Fig. 5.18.

This gives the mode circuit one way time delays as

$$T_1 = 1.410\,605 \text{ ns}$$

$$T_2 = 1.321\,295 \text{ ns}$$

The SPICE program (implemented on the personal computer version, PSPICE) is obtained from the circuit of Fig. 5.19 as

```
SPICE MTL MODEL
VS 1 0 PULSE(0 1 0 6.25N 6.25N 43.75N 100N)
RS 1 2 50
V1 2 3
RL 7 0 50
V3 7 6
RNE 13 0 50
V2 13 12
RFE 8 0 50
V4 8 9
EC1 3 0 POLY(2) (4,0) (11,0) 0 1.118 0.5
EC2 12 0 POLY(2) (4,0) (11,0) 0 -1.234E-5 1.0
EC3 6 0 POLY(2) (5,0) (10,0) 0 1.118,0.5
EC4 9 0 POLY(2) (5,0) (10,0) 0 -1.234E-5 1.0
FC1 0 4 POLY(2) V1 V2 0 1.118 -1.234E-5
FC2 0 11 POLY(2) V1 V2 0 0.5 1.0
```

```
FC3 0 5 POLY(2) V3 V4 0 1.118 -1.234E-5
FC4 0 10 POLY(2) V3 V4 0 0.5 1.0
T1 4 0 5 0 Z0 = 109.354 TD = 1.410605N
T2 11 0 10 0 Z0 = 265.325 TD = 1.321295N
.TRAN .1N 20N 0 .05N
.PRINT TRAN V(2) V(7) V(13) V(8)
.PLOT TRAN V(2) V(7) V(13) V(8)
.END
```

Comparisons with experimentally obtained data will be shown in Section 5.2.6.2.

Another important advantage of the SPICE implementation of the solution is that the *frequency-domain* or *sinusoidal steady-state phasor solution* considered in Chapter 4 can also be obtained from this program with only a slight change in the control statements. These are to redefine the voltage source as

```
VS 1 0 AC 1
```

and redefine the control, print and plot statements as

```
.AC DEC 50 10K 1000MEG
```

(which solves the frequency-domain circuit from 10 kHz to 1 GHz in steps of 50 per decade) and

```
.PRINT AC VM(2) VM(7) VM(13) VM(8)
.PLOT AC VM(2) VM(7) VM(13) VM(8)
```

The remaining statements in the original time-domain program above are unchanged. The above method is implemented in the **SPICEMTL.FOR** digital computer program described in Appendix A. A SPICE subcircuit model is generated by the program which characterizes the MTL at its terminals.

5.2.2 Extension of Branin's Method to Lossless Multiconductor Lines in Homogeneous Media

Branin's method was developed for two-conductor lossless lines. It can be extended in the following manner to *lossless* MTL's in *homogeneous media.* The following extension of that method cannot be readily extended to handle inhomogeneous media. Recall the *frequency-domain* chain parameter matrix as

$$\begin{bmatrix} \hat{\mathbf{V}}(\mathscr{L}) \\ \hat{\mathbf{I}}(\mathscr{L}) \end{bmatrix} = \begin{bmatrix} \hat{\Phi}_{11}(\mathscr{L}) & \hat{\Phi}_{12}(\mathscr{L}) \\ \hat{\Phi}_{21}(\mathscr{L}) & \hat{\Phi}_{22}(\mathscr{L}) \end{bmatrix} \begin{bmatrix} \hat{\mathbf{V}}(0) \\ \hat{\mathbf{I}}(0) \end{bmatrix} \tag{5.78}$$

where the submatrices are given in (4.120) for a *lossless line* in a *homogeneous medium* as

$$\hat{\Phi}_{11} = \cos(\beta\mathscr{L})\mathbf{1}_n \tag{5.79a}$$

$$\hat{\Phi}_{12} = -j\sin(\beta\mathscr{L})\mathbf{Z}_C \tag{5.79b}$$

$$\hat{\Phi}_{21} = -j\sin(\beta\mathscr{L})\mathbf{Z}_C^{-1} \tag{5.79c}$$

$$\hat{\Phi}_{22} = \cos(\beta\mathscr{L})\mathbf{1}_n \tag{5.79d}$$

The characteristic impedance matrix is defined as

$$\mathbf{Z}_C = v\mathbf{L} \tag{5.80a}$$

$$\mathbf{Z}_C^{-1} = v\mathbf{C} \tag{5.80b}$$

and the velocity of propagation is again defined by

$$v = \frac{1}{\sqrt{\mu\varepsilon}} \tag{5.81}$$

The Laplace transform of the corresponding time-domain result can be obtained from this by substituting the Laplace transform variable s for $j\omega$, assuming the line to be initially relaxed, $\mathbf{V}(z, t) = \mathbf{I}(z, t) = \mathbf{0}$ for all $0 \leq z \leq \mathscr{L}$ and $t \leq 0$, and recalling the trigonometric expansions given in (5.11) as

$$\mathbf{V}(\mathscr{L}, s) = \left(\frac{e^{sT} + e^{-sT}}{2}\right)\mathbf{V}(0, s) - \left(\frac{e^{sT} - e^{-sT}}{2}\right)\mathbf{Z}_C\mathbf{I}(0, s) \tag{5.82a}$$

$$\mathbf{I}(\mathscr{L}, s) = -\left(\frac{e^{sT} - e^{-sT}}{2}\right)\mathbf{Z}_C^{-1}\mathbf{V}(0, s) + \left(\frac{e^{sT} + e^{-sT}}{2}\right)\mathbf{I}(0, s) \tag{5.82b}$$

where the line one-way delay is again defined as

$$T = \frac{\mathscr{L}}{v} \tag{5.83}$$

Multiplying (5.82b) by $\mathbf{Z}_C$ and adding and subtracting the equations gives

$$\mathbf{V}(\mathscr{L}, s) + \mathbf{Z}_C\mathbf{I}(\mathscr{L}, s) = e^{-sT}\mathbf{V}(0, s) + e^{-sT}\mathbf{Z}_C\mathbf{I}(0, s) \tag{5.84a}$$

$$\mathbf{V}(\mathscr{L}, s) - \mathbf{Z}_C\mathbf{I}(\mathscr{L}, s) = e^{sT}\mathbf{V}(0, s) - e^{sT}\mathbf{Z}_C\mathbf{I}(0, s) \tag{5.84b}$$

Observing once again the delay transform pair given in (5.9) gives the

time-domain forms as

$$\mathbf{V}(\mathscr{L}, t) + \mathbf{Z}_C\mathbf{I}(\mathscr{L}, t) = \mathbf{V}(0, t - T) + \mathbf{Z}_C\mathbf{I}(0, t - T) \tag{5.85a}$$

$$\mathbf{V}(\mathscr{L}, t) - \mathbf{Z}_C\mathbf{I}(\mathscr{L}, t) = \mathbf{V}(0, t + T) - \mathbf{Z}_C\mathbf{I}(0, t + T) \tag{5.85b}$$

Time shifting (5.85b) and rearranging gives

$$\mathbf{V}(0, t) - \mathbf{Z}_C\mathbf{I}(0, t) = \mathbf{V}(\mathscr{L}, t - T) - \mathbf{Z}_C\mathbf{I}(\mathscr{L}, t - T) \tag{5.85c}$$

Define the vectors

$$\mathbf{E}_i(t - T) = \mathbf{V}(0, t - T) + \mathbf{Z}_C\mathbf{I}(0, t - T) \tag{5.86a}$$

$$\mathbf{E}_r(t - T) = \mathbf{V}(\mathscr{L}, t - T) - \mathbf{Z}_C\mathbf{I}(\mathscr{L}, t - T) \tag{5.86b}$$

The subscripts r and i denote "reflected" and "incident" respectively. Equations (5.85) become

$$\mathbf{V}(\mathscr{L}, t) + \mathbf{Z}_C\mathbf{I}(\mathscr{L}, t) = \mathbf{E}_i(t - T) \tag{5.87a}$$

$$\mathbf{V}(0, t) - \mathbf{Z}_C\mathbf{I}(0, t) = \mathbf{E}_r(t - T) \tag{5.87b}$$

Equations (5.86) time shifted become

$$\mathbf{E}_i(t) = \mathbf{V}(0, t) + \mathbf{Z}_C\mathbf{I}(0, t) \tag{5.88a}$$

$$\mathbf{E}_r(t) = \mathbf{V}(\mathscr{L}, t) - \mathbf{Z}_C\mathbf{I}(\mathscr{L}, t) \tag{5.88b}$$

Substituting (5.87) into (5.88) gives the terminal voltages in terms of the E vectors as

$$\mathbf{V}(0, t) = \tfrac{1}{2}\mathbf{E}_i(t) + \tfrac{1}{2}\mathbf{E}_r(t - T) \tag{5.89a}$$

$$\mathbf{V}(\mathscr{L}, t) = \tfrac{1}{2}\mathbf{E}_r(t) + \tfrac{1}{2}\mathbf{E}_i(t - T) \tag{5.89b}$$

Describe the *resistive terminations* as generalized Thévenin equivalents:

$$\mathbf{V}(0, t) = \mathbf{V}_S(t) - \mathbf{R}_S\mathbf{I}(0, t) \tag{5.90a}$$

$$\mathbf{V}(\mathscr{L}, t) = \mathbf{V}_L(t) + \mathbf{R}_L\mathbf{I}(\mathscr{L}, t) \tag{5.90b}$$

Substituting these terminal relations into (5.88) and using (5.87) gives

$$\mathbf{E}_i(t) = 2\mathbf{M}_S\mathbf{V}_S(t) + \mathbf{\Gamma}_S\mathbf{E}_r(t - T) \tag{5.91a}$$

$$\mathbf{E}_r(t) = 2\mathbf{M}_L\mathbf{V}_L(t) + \mathbf{\Gamma}_L\mathbf{E}_i(t - T) \tag{5.91b}$$

where we have defined, in the fashion for two-conductor lines, the reflection

coefficient matrices as

$$\Gamma_S = (\mathbf{R}_S - \mathbf{Z}_C)(\mathbf{R}_S + \mathbf{Z}_C)^{-1} \tag{5.92a}$$

$$\Gamma_L = (\mathbf{R}_L - \mathbf{Z}_C)(\mathbf{R}_L + \mathbf{Z}_C)^{-1} \tag{5.92b}$$

and the voltage division coefficients are defined as

$$\mathbf{M}_S = \mathbf{Z}_C(\mathbf{R}_S + \mathbf{Z}_C)^{-1} \tag{5.93a}$$

$$\mathbf{M}_L = \mathbf{Z}_C(\mathbf{R}_L + \mathbf{Z}_C)^{-1} \tag{5.93b}$$

The scheme is to discretize the time axis into N computation steps in each one-way time delay T as $\Delta t = T/N$. Then form the four $n \times N$ arrays $\mathbf{E}_l^{\text{OLD}}$, $\mathbf{E}_r^{\text{OLD}}$, $\mathbf{E}_l^{\text{NEW}}$, $\mathbf{E}_r^{\text{NEW}}$. The columns of these are associated with the time increment and the rows are associated with the particular conductor of the line. To begin the recursion algorithm we assume an initially relaxed line and fill $\mathbf{E}_l^{\text{OLD}}$ and $\mathbf{E}_r^{\text{OLD}}$ with zero entries. Then compute the entries in $\mathbf{E}_l^{\text{NEW}}$ and $\mathbf{E}_r^{\text{NEW}}$ according to (5.91) and compute the terminal voltages from (5.89). Once all entries are filled for all time increments for $0 \le t \le T$, write the entries in $\mathbf{E}_l^{\text{NEW}}$ and $\mathbf{E}_r^{\text{NEW}}$ into $\mathbf{E}_l^{\text{OLD}}$ and $\mathbf{E}_r^{\text{OLD}}$ respectively and repeat the calculations for the times in the next interval $T \le t \le 2T$. This is repeated to solve for the terminal voltages in blocks of time of length equal to the one-way line delay, T. This extension of Branin's method to MTLs is implemented in the FORTRAN program **BRANIN.FOR** described in Appendix A. The method implicitly assumes that all modes propagate with the same velocity so that it does not appear feasible to extend it to lines in *inhomogeneous media.*

The recursive method can be solved in series form to give

$$\begin{aligned}\mathbf{V}(0, t) = {} & \mathbf{M}_S\mathbf{V}_S(t) + (\mathbf{1}_n + \Gamma_S)[\Gamma_L\mathbf{M}_S\mathbf{V}_S(t - 2T) + (\Gamma_L\Gamma_S)\Gamma_L\mathbf{M}_S\mathbf{V}_S(t - 4T) \\ & + (\Gamma_L\Gamma_S)^2\Gamma_L\mathbf{M}_S\mathbf{V}_S(t - 6T) + (\Gamma_L\Gamma_S)^3\Gamma_L\mathbf{M}_S\mathbf{V}_S(t - 8T) + \cdots] \\ & + (\mathbf{1}_n + \Gamma_S)[\mathbf{M}_L\mathbf{V}_L(t - T) + (\Gamma_L\Gamma_S)\mathbf{M}_L\mathbf{V}_L(t - 3T) \\ & + (\Gamma_L\Gamma_S)^2\mathbf{M}_L\mathbf{V}_L(t - 5T) + (\Gamma_L\Gamma_S)^3\mathbf{M}_L\mathbf{V}_L(t - 7T) + \cdots]\end{aligned} \tag{5.94a}$$

$$\begin{aligned}\mathbf{V}(\mathscr{L}, t) = {} & \mathbf{M}_L\mathbf{V}_L(t) + (\mathbf{1}_n + \Gamma_L)[\Gamma_S\mathbf{M}_L\mathbf{V}_L(t - 2T) + (\Gamma_S\Gamma_L)\Gamma_S\mathbf{M}_L\mathbf{V}_L(t - 4T) \\ & + (\Gamma_S\Gamma_L)^2\Gamma_S\mathbf{M}_L\mathbf{V}_L(t - 6T) + (\Gamma_S\Gamma_L)^3\Gamma_S\mathbf{M}_L\mathbf{V}_L(t - 8T) + \cdots] \\ & + (\mathbf{1}_n + \Gamma_L)[\mathbf{M}_S\mathbf{V}_S(t - T) + (\Gamma_S\Gamma_L)\mathbf{M}_S\mathbf{V}_S(t - 3T) \\ & + (\Gamma_S\Gamma_L)^2\mathbf{M}_S\mathbf{V}_S(t - 5T) + (\Gamma_S\Gamma_L)^3\mathbf{M}_S\mathbf{V}_S(t - 7T) + \cdots]\end{aligned} \tag{5.94b}$$

These reduce to the exact scalar results for a two-conductor line given in (5.23) but the order of multiplication of the matrices must be preserved here.

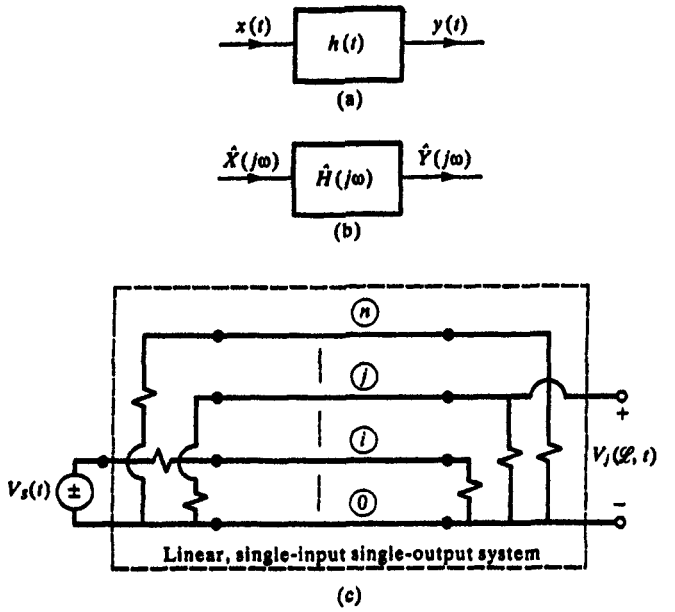

FIGURE 5.20 Illustration of the time-domain to frequency-domain transformation method of computing time-domain responses of *linear* MTLs: (a) a single-input, single-output linear system in the time domain; (b) a single-input, single-output linear system in the frequency domain; and (c) representation of a MTL as a single-input, single-output linear system.

5.2.3 Time-Domain to Frequency-Domain Transformations

Perhaps the most common technique for determining the time-domain response of an MTL is known as the *time-domain to frequency-domain transformation.* This is a straightforward adaptation of a common analysis technique for lumped, linear circuits and systems [A.2]. Consider the *single-input, single-output lumped, linear system* shown in Fig. 5.20(a). The input to the system is denoted as $x(t)$, the output is denoted by $y(t)$, and the *unit impulse response* ($x(t) = \delta(t)$, $y(t) = h(t)$) is denoted by $h(t)$. The independent variable for the lumped system is time, denoted by t. In the time domain, the response is obtained via the *convolution integral* [A.2]:

$$y(t) = \int_{-\infty}^{t} h(t - \tau)x(\tau)\, d\tau \tag{5.95a}$$

which is denoted as

$$y(t) = h(t) * x(t) \tag{5.95b}$$

In the *frequency domain* this translates to

$$\hat{Y}(j\omega) = \hat{H}(j\omega)\hat{X}(j\omega) \tag{5.96}$$

where $\hat{H}(j\omega)$ is the *Fourier transform* of $h(t)$ and is called the *transfer function* of the system as illustrated in Fig. 5.20(b) [A.2]. The frequency-domain transfer function, $\hat{H}(j\omega)$, can be easily obtained by applying unit-magnitude sinusoids to the input and computing the response using the usual *phasor* computational methods with the frequency of those sinusoids varied over the desired frequency range as illustrated in Fig. 5.20(b). Once $\hat{H}(j\omega)$ is obtained in this manner, the time-domain impulse response is obtained as the *inverse Fourier transform* of $\hat{H}(j\omega)$:

$$h(t) = \mathcal{F}^{-1}\{\hat{H}(j\omega)\} \tag{5.97}$$

The method is a very intuitive one. Any time-domain waveform can be decomposed into its sinusoidal components with the Fourier series if it is periodic and the Fourier transform if it is not periodic [A.2]. A periodic waveform with period T has these frequency components appearing at discrete frequencies that are multiples of the basic repetition frequency. If the waveform is nonperiodic, these frequency components appear as a continuum. Nevertheless, the time-domain to frequency-domain method for computing the time-domain response can be described quite simply in the following manner. Decompose the input signal via Fourier methods into its constituent sinusoidal components (magnitude and phase). Pass each component through the system and sum in time the time-domain responses at the output to each of these components by using phasor methods. The magnitudes of the output sinusoidal components are the products of the magnitudes of the input sinusoidal components multiplied by the magnitude of $\hat{H}(j\omega)$ at that frequency. The phases of the output sinusoidal components are the sums of the phases of the input sinusoidal components and the phases of $\hat{H}(j\omega)$ at that frequency. Therefore

$$|\hat{Y}(j\omega_l)| = |\hat{H}(j\omega_l)| \times |\hat{X}(j\omega_l)| \tag{5.98a}$$

$$\underline{/\hat{Y}}(j\omega_l) = \underline{/\hat{H}}(j\omega_l) + \underline{/\hat{X}}(j\omega_l) \tag{5.98b}$$

Clearly *a major restriction on the method is that the system be linear since we are implicitly applying the principle of superposition.*

In the case of a periodic waveform with period T, these frequency components appear at discrete frequencies that are multiples of the basic repetition frequency, $\omega_o = 2\pi f_o = 2\pi/T$, and $x(t)$ can be represented as the sum of these time-domain sinusoidal components with the Fourier series as [A.2]

$$x(t) = c_0 + \sum_{n=1}^{NH} c_n \cos(n\omega_o t + \underline{/c_n}) \tag{5.99}$$

where we have truncated the series to contain only NH harmonics. In the case of a periodic pulse train having trapezoidal pulses of peak magnitude X, duty cycle $D = \tau/T$ where τ is the pulse width (between 50% points), and equal rise/fall times of τ_r, the items in (5.99) become [A.3]:

$$c_0 = XD \tag{5.100a}$$

$$c_n = 2XD \frac{\sin(n\pi D)}{n\pi D} \frac{\sin(n\pi f_o \tau_r)}{n\pi f_o \tau_r} \tag{5.100b}$$

$$\underline{/c_n} = -n\pi(D + f_o\tau_r) \tag{5.100c}$$

For this case of a periodic waveform, we compute the frequency-domain transfer function at *each* of the NH harmonic frequencies with the methods of Chapter 4 (including skin-effect losses if we choose):

$$H(jn\omega_o) = |H(jn\omega_o)|\underline{/H(jn\omega_o)} \tag{5.101}$$

Then multiply each appropriate magnitude and add the angles to give the time domain output as:

$$y(t) = c_0 H(0) + \sum_{n=1}^{NH} c_n |H(jn\omega_o)| \cos(n\omega_o t + \underline{/c_n} + \underline{/H(jn\omega_o)}) \tag{5.102}$$

In this way we can include $\sqrt{f}$ dependent skin-effect losses which are difficult to characterize directly in the time domain as we will discuss in Section 5.3 but again *this supposes a linear system.* This method is implemented in the **FORTRAN program TIMEFREQ.FOR** described in Appendix A. Actually *the periodic waveform results can be used for a nonperiodic waveform if we choose the pulse waveshape over a period to be that of the desired pulse and also choose a repetition frequency low enough that the response reaches its steady-state value before the onset of the next pulse.* This technique is equivalent to avoiding "aliasing" in the application of the fast Fourier transform (FFT).

Consider applying these concepts to a MTL. Suppose we apply a voltage source, $V_S(t)$, to the i-th conductor at $z = 0$ and desire the time-domain response of the j-th line voltage say, at the far end of the line $z = \mathscr{L}$, $V_j(\mathscr{L}, t)$. In order to view this problem as a single-input, single-output system we *imbed* the MTL *along with the terminations* into a two port as illustrated in Fig. 5.20(c) and extract the input to the system, $V_S(t)$, and the output of the system, $V_j(\mathscr{L}, t)$. The frequency-domain transfer function between these two ports, $\hat{H}_{ij}(j\omega)$, can be computed by the phasor methods of Chapter 4 wherein $V_S(t)$ is a sinusoid, $V_S(t) = \sin(\omega t)$. Once the frequency-domain transfer function is obtained in this fashion, the time-domain response can be determined for any time variation of $V_S(t)$ using the above summation of the responses to its sinusoidal components in (5.102) which amounts to the convolution integral of (5.95). An important

advantage is that this method can directly handle frequency-dependent losses such as skin-effect resistance of conductors. Another advantage is that only phasor computational methods are required; there is no need to numerically integrate the time-domain MTL equations. A major disadvantage is that a *linear MTL* is assumed, i.e., the line parameters *and* the terminations are assumed linear. For example, corona breakdown of the surrounding medium as well as nonlinear loads such as diodes and transistors *cannot* be handled with this method since it implicitly assumes a *linear system.* Another disadvantage is that the input signal will consist of a wide spectrum so that accuracy depends on computing the frequency-domain transfer function for what could be a large number of frequencies. Nevertheless, the method is simple to implement for determining the time-domain response of a MTL having *linear terminations.*

5.2.4 Lumped-Circuit Iterative Approximate Characterizations

Lumped-circuit iterative characterizations were discussed in Chapter 4 for approximately characterizing the MTL in the frequency domain. The same circuits can be directly used to characterize the MTL in the time domain but there is an added degree of approximation inherent in their use for time-domain calculations over and above the approximations for the frequency domain. The reader is referred to the structures of these lumped-circuit iterative models, the lumped ⅂, ⌜, π, and T models shown in Fig. 4.12. These structures were developed under the assumption that the MTL was electrically short, $\mathscr{L} \ll \lambda$, *at the frequency under investigation.* In the application of these approximate structures to time-domain calculations, we must recognize that a time-domain input signal contains, in theory, an infinite range of spectral components. So if these structures are used to characterize the time-domain response, those spectral components of the input that are below the frequency where the MTL becomes electrically long will be processed correctly and the higher-frequency components will not be processed correctly. Typically the higher-frequency spectral components contribute to the fine detail of the input (and output) waveshape such as rise and fall times. Incorrectly processing the higher-frequency components will contribute to the "rounding" of the sharp pulse edges. Nevertheless, within this approximation, the lumped-circuit iterative models are simple to use since they may be readily incorporated into any of the various lumped-circuit CAD programs such as SPICE, and the user need only compute the per-unit-length parameters. The FORTRAN program **SPICELPI.FOR** described in Appendix A generates a SPICE subcircuit model for a lumped-pi model of a MTL.

5.2.5 Finite Difference–Time Domain (FDTD) Methods

A common way of approximately determining the time-domain response of a MTL is the use of finite difference–time-domain methods or FDTD [11–13]. The derivatives in the MTL equations are discretized and approximated with

various finite differences. In this method the position variable, z, is discretized as Δz and the time variable, t, is discretized as Δt. There are many ways of approximating the derivatives, $\partial/\partial z$ and $\partial/\partial t$ in those equations [5]. We used a particularly simple discretization in the finite difference method of solving Laplace's equation in two dimensions in Chapter 3.

Consider a real function of one variable, $f(t)$. Expanding this in a Taylor series in a neighborhood of a desired point gives

$$f(t+h) = f(t) + hf'(t) + \frac{h^2}{2!} f''(t) + \frac{h^3}{3!} f'''(t) + \cdots \tag{5.103}$$

where the primes denote the various derivatives with respect to t of the function. Solving this for the first derivative gives

$$f'(t) = \frac{f(t+h) - f(t)}{h} - \frac{h}{2} f''(t) - \frac{h^2}{6} f'''(t) - \cdots \tag{5.104}$$

Thus the first derivative is approximated as

$$f'(t) = \frac{f(t+h) - f(t)}{h} + \mathcal{O}(h) \tag{5.105}$$

where $\mathcal{O}(h)$ denotes that this approximation is valid within an error of order h. So the first derivative may be approximated with the *first-order forward difference*:

$$f'(t) \cong \frac{f(t+h) - f(t)}{h} \tag{5.106}$$

This amounts to approximating the derivative of $f(t)$ using its slope about the region in advance of the desired point. Similarly, the derivative can be approximated as its slope about the region at the desired point by expanding the function $f(t-h)$ with a Taylor series to give

$$f'(t) = \frac{f(t) - f(t-h)}{h} + \frac{h}{2} f''(t) - \frac{h^2}{6} f'''(t) + \cdots \tag{5.107}$$

This gives the *first-order backward difference* accurate to order h:

$$f'(t) \cong \frac{f(t) - f(t-h)}{h} \tag{5.108}$$

Similar approximations for the higher-order derivatives can be found in like

fashion. The second forward difference is

$$f''(t) \cong \frac{f(t+2h) - 2f(t+h) + f(t)}{h^2} \tag{5.109}$$

and the second backward difference is

$$f''(t) \cong \frac{f(t) - 2f(t-h) + f(t-2h)}{h^2} \tag{5.110}$$

both of which are also accurate to within order h.

More accurate approximations known as *central differences* can be found by expanding $f(t+h)$ and $f(t-h)$ in Taylor series as

$$f(t+h) = f(t) + hf'(t) + \frac{h^2}{2!} f''(t) + \frac{h^3}{3!} f'''(t) + \cdots \tag{5.111a}$$

$$f(t-h) = f(t) - hf'(t) + \frac{h^2}{2!} f''(t) - \frac{h^3}{3!} f'''(t) + \cdots \tag{5.111b}$$

Subtracting the equations and solving gives the *first-order central difference*

$$f'(t) \cong \frac{f(t+h) - f(t-h)}{2h} \tag{5.112}$$

which is accurate to order h^2. Similarly, the *second-order central difference* is

$$f''(t) \cong \frac{f(t+h) - 2f(t) + f(t-h)}{h^2} \tag{5.113}$$

which is accurate to order h^2. The discretization of Laplace's equation in the finite difference method of Chapter 3 amounts to a second-order central difference approximation to Laplace's equation. The stability of the solution of Laplace's equation resulting from that discretization is assured, unlike the stability of the discretizations of the transmission-line equations which we now investigate.

Consider the discretization of the transmission-line equations for a two-conductor line. In order to give a general result and to effectively incorporate the terminal conditions we will state these for a lossy line having incident field excitation. This will be covered more completely in Chapter 7 but for the moment, the incident field gives rise to distributed voltage and current sources,

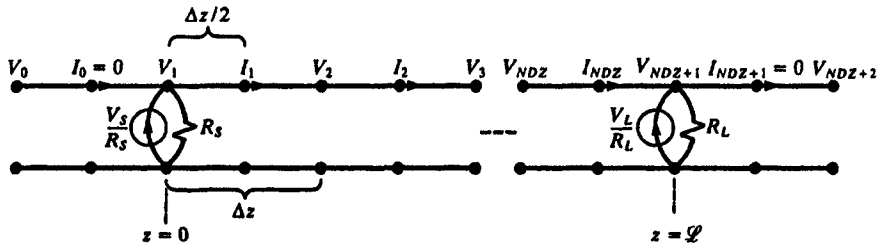

FIGURE 5.21 Illustration of the discretization of a two-conductor line for implementation of the finite difference–time-domain (FDTD) method.

V_F and I_F as

$$\frac{\partial V(z,t)}{\partial z} + l\frac{\partial I(z,t)}{\partial t} + rI(z,t) = V_F(z,t) \tag{5.114a}$$

$$\frac{\partial I(z,t)}{\partial z} + c\frac{\partial V(z,t)}{\partial t} + gV(z,t) = I_F(z,t) \tag{5.114b}$$

We divide the line into NDZ sections each of length Δz as shown in Fig. 5.21. Similarly, we divide the total solution time into segments of length Δt. In order to insure stability of the discretization and to insure second-order accuracy we interlace the $NDZ + 1$ voltage points, $V_1, V_2, \ldots, V_{NDZ}, V_{NDZ+1}$, and the NDZ current points, $I_1, I_2, \ldots, I_{NDZ}$, as shown in Fig. 5.21. Each voltage and adjacent current solution point is separated by $\Delta z/2$. In addition, the time points must also be interlaced and each voltage time point and adjacent current time point are separated by $\Delta t/2$ as illustrated in Fig. 5.22. The second-order, central difference approximations to (5.114) become

$$\frac{V_{k+1}^{n+1} - V_k^{n+1}}{\Delta z} + l\frac{I_k^{n+3/2} - I_k^{n+1/2}}{\Delta t} + r\frac{I_k^{n+3/2} + I_k^{n+1/2}}{2} = \frac{V_{Fk}^{n+3/2} + V_{Fk}^{n+1/2}}{2} \tag{5.115a}$$

$$\frac{I_k^{n+1/2} - I_{k-1}^{n+1/2}}{\Delta z} + c\frac{V_k^{n+1} - V_k^n}{\Delta t} + g\frac{V_k^{n+1} + V_k^n}{2} = \frac{I_{Fk}^{n+1} + I_{Fk}^n}{2} \tag{5.115b}$$

(The superscript n should not be confused with the number of conductors of a general MTL.) The incident field source V_{Fk} is evaluated at the current location I_k, and I_{Fk} is evaluated at the voltage location V_k. Solving these gives the recursion relations:

$$\left(l\frac{\Delta z}{\Delta t} + \frac{r}{2}\Delta z\right)I_k^{n+3/2} = \left(l\frac{\Delta z}{\Delta t} - \frac{r}{2}\Delta z\right)I_k^{n+1/2} - (V_{k+1}^{n+1} - V_k^{n+1}) \tag{5.116a}$$

$$+ \frac{\Delta z}{2}(V_k^{n+3/2} + V_{Fk}^{n+1/2})$$

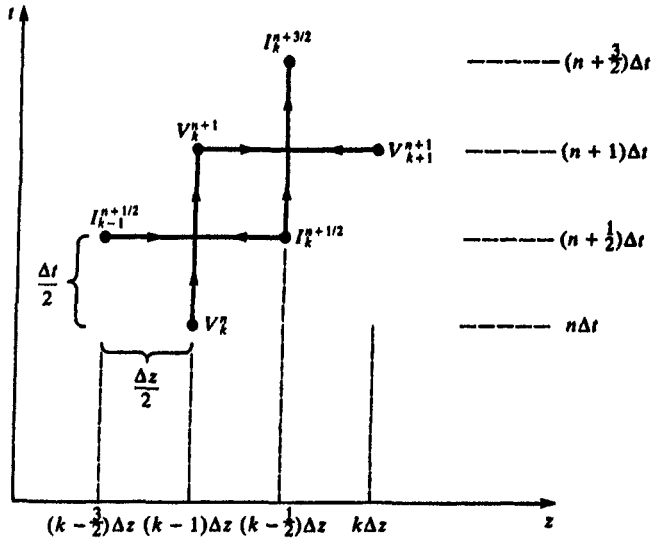

FIGURE 5.22 Illustration of the interlacing of the discrete voltages and currents in position and time to insure stability in the FDTD method.

$$\left(c\frac{\Delta z}{\Delta t}+\frac{g}{2}\Delta z\right)V_k^{n+1}=\left(c\frac{\Delta z}{\Delta t}-\frac{g}{2}\Delta z\right)V_k^n-(I_k^{n+1/2}-I_{k-1}^{n+1/2}) \quad (5.116b)$$
$$+\frac{\Delta z}{2}(I_{Fk}^{n+1}+I_{Fk}^n)$$

These are solved in a "bootstrapping" fashion. First the voltages along the line are solved for a fixed time from (5.116b) in terms of the previous solutions and then the currents are solved for from (5.116a) in terms of these and previous values. The solution starts with an initially relaxed line having zero voltage and current values at all points along the line.

Next consider incorporating the terminal conditions. Referring to Fig. 5.21, represent these as Norton equivalents where we allow for lumped sources and loads at $z = 0$, characterized by $I_S = V_S/R_S$ and R_S, and at $z = \mathscr{L}$, characterized by $I_L = V_L/R_L$ and R_L. We will show that the exact way of incorporating these terminal constraints is to substitute into (5.116b) for $k = 1$:

$$I_0 = 0 \quad (5.117a)$$

$$g = \frac{1}{R_S \Delta z} \quad (5.117b)$$

$$I_{Fk} = \frac{V_S}{R_S \Delta z} \quad (5.117c)$$

Similarly we impose the terminal constraints at $z = \mathscr{L}$ by substituting into (5.116b) for $k = NDZ + 1$:

$$I_{NDZ+1} = 0 \tag{5.118a}$$

$$g = \frac{1}{R_L \Delta z} \tag{5.118b}$$

$$I_{Fk} = \frac{V_L}{R_L \Delta z} \tag{5.118c}$$

We will also show that setting $I_0 = I_{NDZ+1} = 0$ $k = 1$ and $k = NDZ + 1$ in (5.116b) requires that we replace $c\Delta z$ with $c\Delta z/2$ in *only those two equations.* Equation (5.116b) for all other k, $k = 2, 3, \ldots, NDZ$, must use $c\Delta z$. In this section we will consider lossless lines so we set

$$r = V_{Fk} = 0 \tag{5.119a}$$

in (5.116a) for all k and set

$$g = I_{Fk} = 0 \tag{5.119b}$$

in (5.116b) for $k = 2, 3, \ldots, NDZ$. This gives the final difference equations to be solved. Equation (5.116b) for $k = 1$:

$$\begin{aligned} V_1^{n+1} &= \left(R_S \frac{c}{2}\frac{\Delta z}{\Delta t} + \frac{1}{2}\right)^{-1} \\ &\quad \times \left[\left(R_S \frac{c}{2}\frac{\Delta z}{\Delta t} - \frac{1}{2}\right) V_1^n - R_S\left(I_1^{n+1/2} \underbrace{- I_0^{n+1/2}}_{=0}\right) + \frac{(V_S^{n+1} + V_S^n)}{2}\right] \\ &= \left(R_S \frac{c}{2}\frac{\Delta z}{\Delta t} + \frac{1}{2}\right)^{-1} \\ &\quad \times \left[\left(R_S \frac{c}{2}\frac{\Delta z}{\Delta t} - \frac{1}{2}\right) V_1^n - R_S(I_1^{n+1/2}) + \frac{(V_S^{n+1} + V_S^n)}{2}\right] \end{aligned} \tag{5.120a}$$

Equation (5.116b) for $k = 2, 3, \ldots, NDZ$:

$$V_k^{n+1} = V_k^n - \frac{\Delta t}{\Delta z} c^{-1}(I_k^{n+1/2} - I_{k-1}^{n+1/2}) \tag{5.120b}$$

Equation (5.116b) for $k = NDZ + 1$:

$$V_{NDZ+1}^{n+1} = \left(R_L \frac{c}{2}\frac{\Delta z}{\Delta t} + \frac{1}{2}\right)^{-1} \tag{5.120c}$$
$$\times \left[\left(R_L \frac{c}{2}\frac{\Delta z}{\Delta t} - \frac{1}{2}\right) V_{NDZ+1}^{n} - R_L\left(\underbrace{I_{NDZ+1}^{n+1/2}}_{=0.} - I_{NDZ}^{n+1/2}\right) + \frac{(V_L^{n+1} + V_L^n)}{2}\right]$$
$$= \left(R_L \frac{c}{2}\frac{\Delta z}{\Delta t} + \frac{1}{2}\right)^{-1}$$
$$\times \left[\left(R_L \frac{c}{2}\frac{\Delta z}{\Delta t} - \frac{1}{2}\right) V_{NDZ+1}^{n} + R_L(I_{NDZ}^{n+1/2}) + \frac{(V_L^{n+1} + V_L^n)}{2}\right]$$

Equation (5.116a) for $k = 1, 2, \ldots, NDZ$:

$$I_k^{n+3/2} = I_k^{n+1/2} - \frac{\Delta t}{\Delta z} l^{-1}(V_{k+1}^{n+1} - V_k^{n+1}) \tag{5.120d}$$

The voltages and currents are solved by iterating k for a fixed time (solving first for the voltages and then for the currents) and then iterating time. The initial conditions of zero voltage and current are used to start the iteration. The conditions for this set of recursion relations to be stable is the Courant condition:

$$\Delta t \leq \frac{\Delta z}{v} \tag{5.121}$$

which amounts to the condition that the time step must be no greater than the propagation time over each cell. The Δz discretization is chosen sufficiently small such that each Δz section is *electrically small* at the significant spectral components of the source voltages, $V_S(t)$ and $V_L(t)$.

It is not obvious that the method of incorporating the terminal constraints by using the distributed conductance, g, and distributed induced field source, I_F, in (5.115b) or (5.116b) and making the correspondences as in (5.117) and (5.118) properly incorporates these lumped loads. Nor is it obvious that we must use $c\Delta z/2$ in the end sections and $c\Delta z$ in the interior sections in (5.116b). We will now prove this and, in addition, will show that if we choose the time and position discretizations such that

$$\Delta t = \frac{\Delta z}{v} \tag{5.122}$$

(which is sometimes referred to as the "magic time step"), the above difference equations will yield the *exact solution* with no approximation error! In order

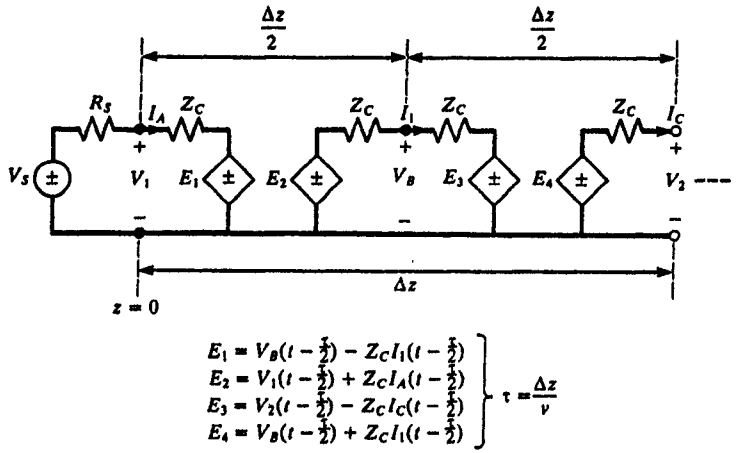

FIGURE 5.23 Use of Branin's equivalent circuit to prove the exactness of the FDTD voltage recursion relation at the source.

to show this let us model the source end of the line for the first section of length Δz using the exact time-delay model of Branin's method as shown in Fig. 5.23. The voltages and current to be solved for in the finite difference solution are V_1, I_1, V_2. The currents and voltage I_A, V_B, I_C are auxiliary variables and are not solved for in the finite difference method. Each half of length $\Delta z/2$ is modeled with its own exact solution with reference to Fig. 5.8 with time delay of $\tau/2$ where

$$\tau = \frac{\Delta z}{v} \tag{5.123}$$

In order to simplify the derivation, we again use the *difference operator*:

$$D^{\pm m} f(t) = f(t \pm m\tau) \tag{5.124}$$

The resulting equations relating all voltages and currents in Fig. 5.23 are

$$V_1 = Z_C I_A + D^{-1/2}(V_B - Z_C I_1) \tag{5.125a}$$

$$V_B = -Z_C I_1 + D^{-1/2}(V_1 + Z_C I_A) \tag{5.125b}$$

$$V_B = Z_C I_1 + D^{-1/2}(V_2 - Z_C I_C) \tag{5.125c}$$

$$V_2 = -Z_C I_C + D^{-1/2}(V_B + Z_C I_1) \tag{5.125d}$$

The objective here is to eliminate I_A, V_B, I_C from these equations and write the

result in terms of V_1, I_1, V_2. The terminal constraints at $z = 0$ are

$$I_A = \frac{V_S}{R_S} - \frac{V_1}{R_S} \tag{5.126}$$

Substituting (5.126) into (5.125a) and (5.125b) gives

$$V_1 = \frac{Z_C}{R_S} V_S - \frac{Z_C}{R_S} V_1 + D^{-1/2}(V_B - Z_C I_1) \tag{5.127a}$$

$$V_B = -Z_C I_1 + D^{-1/2}\left(V_1 + \frac{Z_C}{R_S} V_S - \frac{Z_C}{R_S} V_1\right) \tag{5.127b}$$

Operating on (5.127a) with D and (5.127b) with $D^{1/2}$ and substituting gives

$$\left(1 + \frac{Z_C}{R_S}\right) DV_1 = \left(1 - \frac{Z_C}{R_S}\right) V_1 - 2Z_C D^{1/2} I_1 + \frac{Z_C}{R_S}(DV_S + V_S) \tag{5.128}$$

Rewriting (multiply both sides by $R_S/2Z_C$) gives

$$DV_1 = \left(\frac{1}{2}\frac{R_S}{Z_C} + \frac{1}{2}\right)^{-1}\left[\left(\frac{1}{2}\frac{R_S}{Z_C} - \frac{1}{2}\right) V_1 - R_S D^{1/2} I_1 + \frac{1}{2}(DV_S + V_S)\right] \tag{5.129}$$

$$= \Gamma_S V_1 - 2\frac{Z_C R_S}{Z_C + R_S} D^{1/2} I_1 + \frac{Z_C}{Z_C + R_S}(DV_S + V_S)$$

where we have written this result in terms of the source reflection coefficient, Γ_S. In order to show that (5.129) is equivalent to (5.120a) for the magic time step of (5.122), we substitute (5.122) along with the fundamental relation between the per-unit-length capacitance and the characteristic impedance, $vc = Z_C^{-1}$, into (5.120a) which gives (5.129). This shows that (5.120a) is the proper finite difference relation for the end section and that for this section we must use $c\Delta z/2$ rather than $c\Delta z$!

Similarly we may draw the exact circuit for the last Δz section as shown in Fig. 5.24. The equations are

$$V_{NDZ} = Z_C I_A + D^{-1/2}(V_B - Z_C I_{NDZ}) \tag{5.130a}$$

$$V_B = -Z_C I_{NDZ} + D^{-1/2}(V_{NDZ} + Z_C I_A) \tag{5.130b}$$

$$V_B = Z_C I_{NDZ} + D^{-1/2}(V_{NDZ+1} - Z_C I_C) \tag{5.130c}$$

$$V_{NDZ+1} = -Z_C I_C + D^{-1/2}(V_B + Z_C I_{NDZ}) \tag{5.130d}$$

The objective is to incorporate the lumped terminal conditions at $z = \mathscr{L}$ and to eliminate I_A, V_B, I_C to give an equation in V_{NDZ}, I_{NDZ}, V_{NDZ+1} which, for the

Next Page

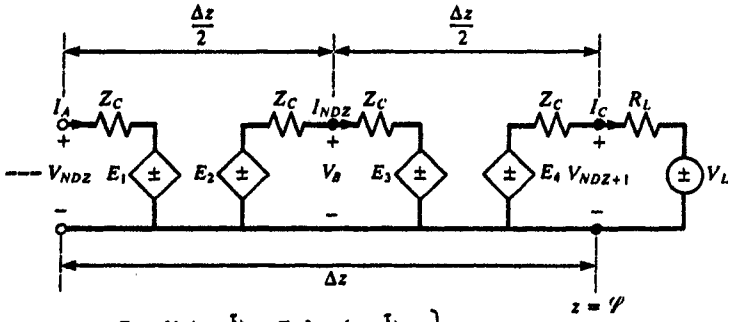

$$\left.\begin{aligned} E_1 &= V_B(t-\tfrac{1}{2}) - Z_C I_{NDZ}(t-\tfrac{1}{2}) \\ E_2 &= V_{NDZ}(t-\tfrac{1}{2}) + Z_C I_A(t-\tfrac{1}{2}) \\ E_3 &= V_{NDZ+1}(t-\tfrac{1}{2}) - Z_C I_C(t-\tfrac{1}{2}) \\ E_4 &= V_B(t-\tfrac{1}{2}) + Z_C I_{NDZ}(t-\tfrac{1}{2}) \end{aligned}\right\} \tau = \frac{\Delta z}{v}$$

FIGURE 5.24 Use of Branin's equivalent circuit to prove the exactness of the FDTD voltage recursion relation at the load.

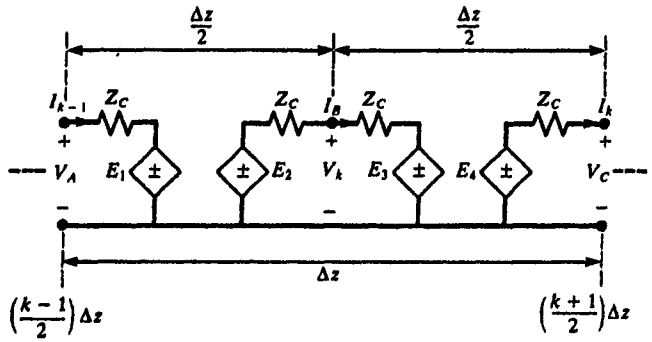

$$\left.\begin{aligned} E_1 &= V_k(t-\tfrac{1}{2}) - Z_C I_B(t-\tfrac{1}{2}) \\ E_2 &= V_A(t-\tfrac{1}{2}) + Z_C I_{k-1}(t-\tfrac{1}{2}) \\ E_3 &= V_C(t-\tfrac{1}{2}) - Z_C I_k(t-\tfrac{1}{2}) \\ E_4 &= V_k(t-\tfrac{1}{2}) + Z_C I_B(t-\tfrac{1}{2}) \end{aligned}\right\} \tau = \frac{\Delta z}{v}$$

FIGURE 5.25 Use of Branin's equivalent circuit to prove the exactness of the FDTD voltage recursion relation at an intermediate point on the line.

magic time step of (5.122) is equivalent to (5.120c). Again this can be readily done as above.

The remaining tasks are to show that (5.120b) and (5.120d) are correct for the magic time step. First we show that (5.120b) is correct by representing a Δz section containing I_{k-1}, V_k, I_k with the exact Branin's model as shown in Fig. 5.25. The equations from that model are

$$V_A = Z_C I_{k-1} + D^{-1/2}(V_k - Z_C I_B) \tag{5.131a}$$